CONVERGENCE-RATE AND ERROR ANALYSIS OF SECTIONAL-VOLUME AVERAGE METHOD FOR THE COLLISIONAL BREAKAGE EQUATION WITH MULTI-DIMENSIONAL MODELLING

PRAKRATI KUSHWAH, ANUPAMA GHORAI, AND JITRAJ SAHA

ABSTRACT. Recent literature reports two sectional techniques, the finite volume method [Das et al., 2020, SIAM J. Sci. Comput., 42(6): B1570-B1598] and the fixed pivot technique [Kushwah et al., 2023, Commun. Nonlinear Sci. Numer. Simul., 121(37): 107244] to solve one-dimensional collision-induced nonlinear particle breakage equation. It is observed that both the methods become inconsistent over random grids. Therefore, we propose a new birth modification strategy, where the newly born particles are proportionately allocated in three adjacent cells, depending upon the average volume in each cell. This modification technique improves the numerical model by making it consistent over random grids. A detailed convergence and error analysis for this new scheme is studied over different possible choices of grids such as uniform, nonuniform, locally-uniform, random and oscillatory grids. In addition, we have also identified the conditions upon kernels for which the convergence rate increases significantly and the scheme achieves second order of convergence over uniform, nonuniform and locally-uniform grids. The enhanced order of accuracy will enable the new model to be easily coupled with CFD-modules. Another significant advancement in the literature is done by extending the discrete model for two-dimensional equation over rectangular grids.

1. INTRODUCTION

In disperse system, particles are encountered by several physical processes such as aggregation, breakage, nucleation, evaporation etc. The particle encounters can be induced by some external force or due to Brownian motion among the fellow particles. During such encounters, particles disintegrate into smaller fragments, thus leading to the breakage process.

Thus, particle volume evolves in a closed system over a period of time and the equations representing these mechanisms are called breakage population balance equations (PBEs). PBEs are initial valued integro-partial differential equations. Mathematical model where breakage PBEs are induced by external force is represented by a linear equation [16]. On the other hand, mathematical model for breakage PBEs, driven by the collisions between particles is nonlinear equation [11]. Note that the collisions between two mother particles can lead to an outcome in which one mother particle breaks into smaller fragments while other remains unchanged, acting as a catalyst. This study focuses on the collision-induced nonlinear breakage process that has several applications in real life. The collision-induced breakage process can be experienced during the formation of raindrops and bubbles. Prat et al. [15] have identified that during the formation of raindrop and bubbles, the collisions occur among the raindrops (which can also be treated as particles) and raindrops disintegrate into smaller ones. They have modeled this phenomena with the help of the discrete nonlinear equation and explored the solution (which is the raindrop size distribution) through Monte Carlo simulations. On a furthernote, the collisional nonlinear breakage equation plays crucial role for productions of powders with particular density distribution for drug formation and to create specified sizes tablets from wet granulation process [17]. Various other applications of such breakage model are found in dense disperse system for fluidized beds [13], astrophysics [14], the crushing or milling processing, mineral processing, material science and both batch and continuous granulation processes.

1.1. The continuous collisional nonlinear breakage model.
In this article, we consider the continuous collision-induced nonlinear breakage equation which is first introduced by Cheng and Redner [1, 2]. The time evolution of density distribution function $n(x, t)$ of particles of volume $x \geq 0$ at time $t \geq 0$ due to the

collision induced breakage process is governed by the following equation:

$$(1.1) \qquad \frac{\partial n(x,t)}{\partial t} = \int_0^\infty \int_x^\infty \beta(x|y;z)\mathcal{K}(y,z)n(y,t)n(z,t)\mathrm{d}y\mathrm{d}z - \int_0^\infty \mathcal{K}(x,y)n(x,t)n(y,t)\mathrm{d}y,$$

with the initial condition

$$(1.2) \qquad n(x,0) = n_0(x) \geq 0, \quad \text{for any} \quad x \geq 0.$$

Here, functions $\beta(x|y;z)$ and $\mathcal{K}(y,z)$ are the breakage distribution function and the collisional rate kernel respectively. The first term on the right hand side (R.H.S.) of (1.1) is the birth term which represents the formation of x volume particles as a result of collision between two particles of y $(> x)$ and z volume. The mother particle of y volume breaks into the smaller particle of volume x whereas particle of volume z acts like a catalyst and remain unchanged during collision. The second term on R.H.S. of (1.1) is the death term that accounts the depletion of particles of volume x from the system. In general, the collisional kernel and the breakage distribution function satisfies the following properties:
(i) $\mathcal{K}(y,z)$ is nonnegative and symmetric with respect to the arguments y and z i.e. satisfies the conditions,

$$(1.3) \qquad 0 \leq \mathcal{K}(y,z) = \mathcal{K}(z,y), \quad \text{for all} \quad y,z > 0,$$

(ii) $\beta(x|y;z)$ is nonnegative satisfying the condition $\beta(x|y;z) = 0$ when $x > y$ and the volume conserving property,

$$(1.4) \qquad \int_0^y x\beta(x|y;z)\mathrm{d}x = y, \quad \text{for all} \quad y,z > 0,$$

and total number of fragments produced during a breakage event is calculated as

$$(1.5) \qquad \int_0^y \beta(x|y;z)\mathrm{d}x = \zeta(y,z), \quad \text{where} \quad 2 \leq \zeta(y,z) \leq \bar{\zeta} < \infty, \quad \text{for all} \quad y,z > 0.$$

For population balance equations, conservation of particles properties such as mass and number of particles of the system plays a key role to determine the density evolution for certain kinetic rates. In this regard, some integral properties of the density function play a crucial role to indicate several significant physical properties. For this purpose, the rth order moment is denoted by $\mathcal{M}_r(t)$ and is defined by

$$(1.6) \qquad \mathcal{M}_r(t) = \int_0^\infty x^r n(x,t)\mathrm{d}x \quad \text{for all} \quad t \geq 0 \text{ and } r = 0,1,2,\ldots\ldots$$

Consider, a function $\varphi(x)$ of positive real numbers. Now, multiplying the breakage equation (1.1) with $\varphi(x)$ on both sides and taking integration over x, we obtain the corresponding moment equation for the collisional nonlinear breakage equation

$$(1.7) \qquad \frac{\mathrm{d}}{\mathrm{d}t}\int_0^\infty \varphi(x)n(x,t)\mathrm{d}x = \int_0^\infty \int_0^\infty \left(\int_0^y \varphi(x)\beta(x|y;z)\mathrm{d}x - \varphi(y)\right)\mathcal{K}(y,z)n(y,t)n(z,t)\mathrm{d}y\mathrm{d}z.$$

Setting $\varphi(x) = 1$ in equation (1.7) and using property (1.5), we obtain the time evolution of zeroth moment given as

$$(1.8) \qquad \frac{\mathrm{d}\mathcal{M}_0(t)}{\mathrm{d}t} = \int_0^\infty \int_0^\infty [\zeta(y,z) - 1]\,\mathcal{K}(y,z)n(y,t)n(z,t)\mathrm{d}y\mathrm{d}z.$$

Likewise, setting $\varphi(x) = x$ in equation (1.7) and by property (1.5), we obtain the time evolution of the first moment of the particles as

$$\frac{\mathrm{d}\mathcal{M}_1(t)}{\mathrm{d}t} = 0 \text{ implies } \mathcal{M}_1(t) = \mathcal{M}_1(0), \text{ for all } t \geq 0.$$

provided all the integrals in the R.H.S. of equation (1.7) exists. Thus, for a suitable choice of kinetic rates the volume conservation law holds appropriately.

1.2. **The state of art and motivation.** The evolution of raindrop size distribution undergoing the colli-
sion induced nonlinear breakage process [15, 18] is extensively used to describe the precipitation dynamics,
weather modeling, and radar meteorology. Moreover, several other applications in real life and industrial
processes urge researchers to explore more on the collisional nonlinear breakage equation. In literature, this
equation is mostly theoretically analysed [6, 7] and less numerically investigated. Since achieving analytical
solutions of the collisional nonlinear breakage equation is very challenging, so the primary motivation lies
on securing efficient numerical solutions. In this regard, various numerical methods including sectional dis-
cretization methods [3, 11], Monte Carlo simulations [5] and semi-analytical methods [19] are implemented
in the literature to solve the collisional nonlinear breakage equation. Among these numerical methods, the
sectional discretization methods are formulated on the basis of distributing the particles in the represen-
tatives as well as neighboring nodes (or pivots) for capturing the required integral properties accurately.
Monte Carlo method needs a significant large number of data to achieve higher accuracy, thus involving a
significant computational cost. On the other hand, semi-analytical method uses the analytical toolbox of the
supporting software and hence very slow to produce results for higher iterations. Additionally, this method
fails to give solution of any complex, nonlinear equations in closed form except specific conditions. Thus,
the sectional discretization methods are efficient to address and overcome these limitations for generating
results with better accuracy. In last few decades, these section based methods includes finite volume methods
(FVM) [4,8], fixed pivot techniques (FPT) [9,16] and cell average techniques (CAT) [10,12] to solve the linear
breakage equation. In recent literature, there are few works documented to address the numerical treatment
of the collisional nonlinear breakage equation, employing sectional discretization methods including FVM [3]
and FPT [11] to solve the equation (1.1) but these existing schemes have its limitations. For FVM, the
allocation of the new born particles is restricted to a single pivot whereas in FPT, two pivots are used for
birth modification. Moreover, FVM is highly acccurate for a particular choice of grids that is the geometric,
but for other choice of grids it struggles with performance. Additionally, FVM fails on coarser grids. On the
other hand, FPT offers some definite improvement, yet it fails over randomly generated grids. For overall
accuracy, it achieves first order convergence rate. In this context, we propose an improved sectional dis-
cretization method based on particles averaged volume in a particular cell named as *volume average method*
(VAM). The cell allocation is done in three nighboring cells based on the properties of particles volume
average, which are expected to be preserved. The birth terms are modified in order to achieve consistency
with total volume and number of particles. The nonnegative solution obtained from the numerical scheme
and consistency of the scheme are examined in detail followed by a discussion on discretization error over
different grid types. It is observed that VAM is first order convergent over uniform, nonuniform and locally-
uniform grids. Most significant observation is that VAM shows first order convergent over random grids. We
also study the performance of VAM over oscillatory grids which is first evidence where consistency analysis
is reported for the collisional nonlinear breakage equation in the literature and this new method achieves
first order accurate. An important observation is discussed where conditions depending upon the kernels
for which the VAM shows second order convergence over uniform, nonuniform and locally-uniform grids and
maintains first order accuracy over random and oscillatory grids. The accuracy of the new scheme VAM is
validated against the existing fixed pivot technique. It is worth mentioning here that the existing FPT is
inconsistent over random grids. Furthermore, we carry out the stability analysis of the new scheme using
Lipschitz criterion. The model is further extended for two-dimensional case over the rectangular grids. For
numerical results, two examples are solved, where the total particle properties and the particle hypervolume
are calculated against their exact values. Importantly, the results show that VAM performs better than the
existing FPT.

The article is organized as follows: in section 2, we describe the cell adaptive mathematical formulation
of VAM for the collisional nonlinear breakage equation (1.1). Section 3 discusses the convergence and
consistency analysis. Two-dimensional model is presented in section 4 and numerical discussion is done for
different text problems in section 5. The findings of the work are highlighted in section 6.

2. The cell volume average method

We first truncate the continuous collisional breakage equation (1.1) by considering a finite computational domain as $\Lambda = [0, x_{\max}]$ with $x_{\max} < \infty$: for all $x \in \Lambda$ and $t \geq 0$ and the truncated equation (1.1) reads as

$$(2.1) \qquad \frac{\partial n(x,t)}{\partial t} = \int_0^{x_{\max}} \int_x^{x_{\max}} \beta(x|y;z)\mathcal{K}(y,z)n(y,t)n(z,t)\mathrm{d}y\mathrm{d}z - \int_0^{x_{\max}} \mathcal{K}(x,y)n(x,t)n(y,t)\mathrm{d}y,$$

with the initial condition

$$(2.2) \qquad n(x,0) = n_0(x) \quad \text{for any} \quad x \in \Lambda.$$

We now discretize the volume domain Λ into $I(< \infty)$ discrete cells. Let Λ_i denotes the ith cell, $\Lambda_i := [x_{i-1/2}, x_{i+1/2}]$ with $x_{1/2} := 0$ and $x_{I+1/2} := x_{\max}$ and $\Delta x_i := x_{i+1/2} - x_{i-1/2}$. A finitely discretized computational domain is shown in Figure 1. The midpoint $x_i := \dfrac{x_{i+1/2} + x_{i-1/2}}{2}$ of Λ_i is the cell representatives or pivots. It is assumed that the particle property is concentrated at these pivots. Consider $\Delta x_i \leq \Delta x_{i+1}$ and $\Delta x_{\min} = \min_i \Delta x_i \leq \Delta x_i \leq \Delta x = \max_i \Delta x_i$ with $\dfrac{\Delta x}{\Delta_{\min}} \leq \alpha$, a constant, for all $1 \leq i \leq I$. Let $N_i(t)$ be the discrete number density in the ith cell at time t defined by

$$(2.3) \qquad N_i(t) = \int_{x_{i-1/2}}^{x_{i+1/2}} n(x,t)\mathrm{d}x.$$

Using relation $n(x,t) \approx \sum_{i=1}^{I} N_i(t)\delta(x-x_i)$ in the truncated equation (2.1), we obtain the collisional nonlinear breakage equation as

$$(2.4) \qquad \frac{\mathrm{d}N_i(t)}{\mathrm{d}t} = \hat{B}_i(t) - \hat{D}_i(t), \quad \text{with initial conditions} \quad N_i(0) = N_i^0,$$

for all $i = 1, 2, \ldots, I$. Here, birth terms and death terms are defined as respectively

$$(2.5) \qquad \hat{B}_i(t) = \sum_{k=1}^{I} \sum_{j=i}^{I} \beta_{i,j}^k \mathcal{K}(x_j, x_k) N_j(t) N_k(t) \quad \text{and} \quad \hat{D}_i(t) = \sum_{j=1}^{I} \mathcal{K}(x_i, x_j) N_i(t) N_j(t),$$

with

$$(2.6) \qquad \beta_{i,j}^k = \int_{x_{i-1/2}}^{p_j^i} \beta(x|x_j; x_k)\mathrm{d}x \quad \text{and} \quad p_j^i = \begin{cases} x_i, & \text{if} \quad i = j, \\ x_{i+1/2}, & \text{otherwise.} \end{cases}$$

Note that positivity of all the terms appearing on the R.H.S. of $B_i(t)$ and $D_i(t)$ defines positivity of the both $B_i(t)$ and $D_i(t)$. The rth order discrete moment is defined as $\hat{\mathcal{M}}_r(t) = \sum_{i=1}^{I} x_i^r N_i(t)$, for all $r \in \mathbb{N}$. Recalling equation (1.7) the discrete moment equation is written as

$$(2.7) \qquad \frac{\mathrm{d}}{\mathrm{d}t} \sum_{i=1}^{I} \varphi_i N_i(t) = \sum_{k=1}^{I} \sum_{j=1}^{I} \mathcal{K}(x_j, x_k) N_j(t) N_k(t) \left(\sum_{i=1}^{j} \int_{x_{i-1/2}}^{p_i^j} \varphi_i \beta(x|x_j; x_k)\mathrm{d}x - \varphi_j \right),$$

where $\{\varphi_i\}_{i \geq 1}$ is a sequence of positive real numbers. Consequently, setting $\varphi_i = 1$ and x_i in equation (2.7), the time evolution of the discrete zeroth moment and first moment are written as respectively

$$(2.8) \qquad \frac{\mathrm{d}\hat{\mathcal{M}}_0(t)}{\mathrm{d}t} = \sum_{k=1}^{I} \sum_{j=1}^{I} \mathcal{K}(x_j, x_k) N_j(t) N_k(t) \left[\zeta(x_j, x_k) - 1 \right],$$

and

$$(2.9) \qquad \frac{\mathrm{d}\hat{\mathcal{M}}_1(t)}{\mathrm{d}t} = \sum_{k=1}^{I} \sum_{j=1}^{I} \mathcal{K}(x_j, x_k) N_j(t) N_k(t) \left(\sum_{i=1}^{j} \int_{x_{i-1/2}}^{p_i^j} x_i \beta(x|x_j; x_k)\mathrm{d}x - x_j \right).$$

Remark 2.1. The discrete formulation (2.4) is not consistent with discrete first order moment. [5]

Since the discrete formulation (2.4) fails to preserve the total mass of the particles in system, it is not suitable to approximate the collisional nonlinear breakage equation (1.1). To overcome this limitation, we formulate a new numerical method which modifies the birth term of equation (1.1) and conserves the total mass as well as number of the particles.

2.1. **Cell volume average based birth rate modification.** To capture the birth rate of the particles more precisely, the daughter particles are assigned to the neighboring pivots depending upon the position of the average volume $\bar{v}_i$ in Λ_i. In this context, to obtain the average volume, the discrete volume flux over Λ_i is defined as

$$(2.10) \qquad \hat{V}_i(t) = \sum_{k=1}^{I}\sum_{j=i}^{I} \mathcal{K}(x_j, x_k)N_j(t)N_k(t)\int_{x_{i-1/2}}^{p_j^i} x\beta(x|x_j; x_k)\mathrm{d}x,$$

and recalling $B_i(t)$ from equation (2.5) the volume average $\bar{v}_i$ of all newborn particles in Λ_i as

$$(2.11) \qquad \bar{v}_i = \frac{\hat{V}_i(t)}{\hat{B}_i(t)}, \quad \text{for all} \quad i = 1, 2, \ldots, I.$$

There are two possibilities for the particle allocation in a cell as follows:

(1) (Less likely event) if the average volume $\bar{v}_i$ of the particles in Λ_i matches with the volume of cell representative (happens very rarely) i.e. $\bar{v}_i = x_i$, then the total birth B_i can be allocated to the node x_i. Here, all properties corresponding to the average volume of particles are preserved trivially.
(2) (Most likely event) if the average volume $\bar{v}_i$ of the particles in Λ_i does not match with the volume of cell representative, that is either $\bar{v}_i > x_i$ or $\bar{v}_i < x_i$, then the particles are distributed to the neighboring pivots such that the total number of particles and mass are preserved. Then, depending upon the position of average volume, we see the contribution of fractions of birth term in the neighboring pivots.
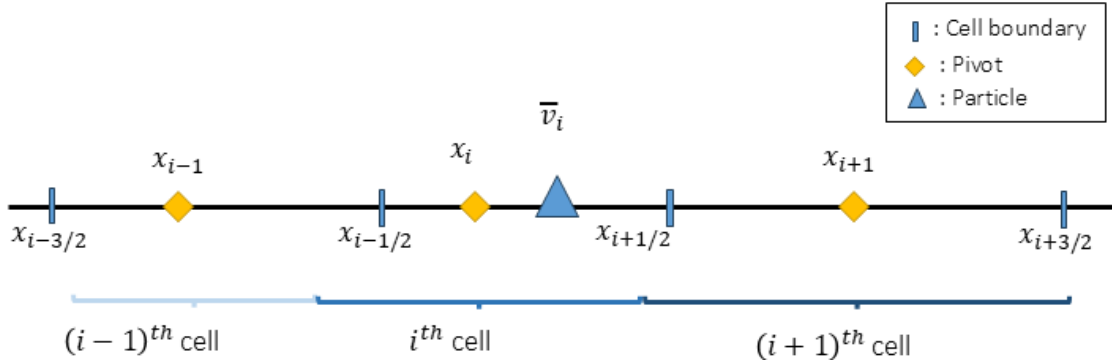

FIGURE 1. Particle allocation

Consider $\bar{v}_i > x_i$ (see Figure 1) and x_i and x_{i+1} are the two neighboring nodes associated with $\bar{v}_i$. Consider the terms $c_1(\bar{v}_i, x_i)$ and $c_2(\bar{v}_i, x_{i+1})$ are the fractions of the birth terms $\hat{B}_i(t)$ to be allocate at x_i and x_{i+1} respectively. Then, to preserve number of particles and volume allocated in i and $i + 1$ cell, the fractions should satisfy the following relations:

$$(2.12) \qquad c_1(\bar{v}_i, x_i) + c_2(\bar{v}_i, x_{i+1}) = \hat{B}_i \quad \text{and} \quad x_i c_1(\bar{v}_i, x_i) + x_{i+1}c_2(\bar{v}_i, x_{i+1}) = \bar{v}_i\hat{B}_i.$$

Solving relations (2.12), we get

$$(2.13) \qquad c_1(\bar{v}_i, x_i) = \hat{B}_i\lambda_i^+(\bar{v}_i) \quad \text{and} \quad c_2(\bar{v}_i, x_{i+1}) = \hat{B}_i\lambda_{i+1}^-(\bar{v}_i), \quad \text{where} \quad \lambda_i^\pm(x) = \frac{x - x_{i\pm1}}{x_i - x_{i\pm1}}.$$

Now, there arise four possible birth fractions that can be considered during a birth assignment at x_i. Among these, two birth fractions arise from the ith cell and other two arise from the neighboring cells (see Figure 2).
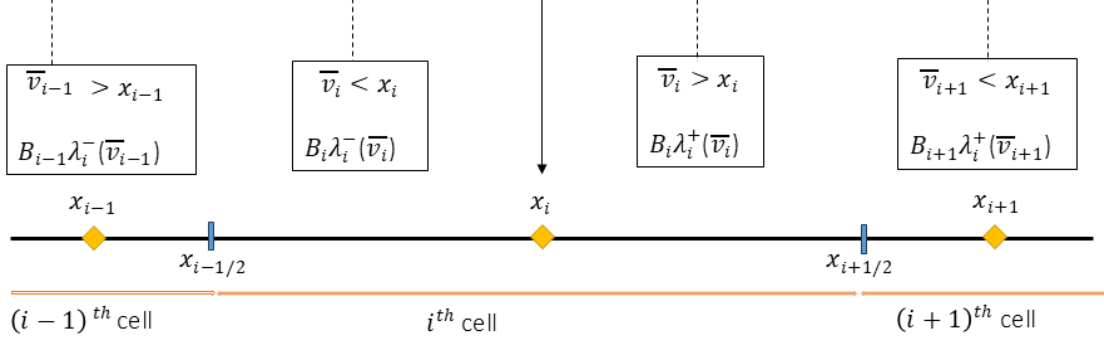
FIGURE 2. Particle contribution at x_i from all possible cells

Considering all possible birth assignments, the following semi-discrete system obtained due to cell volume average method is defined as

$$(2.14) \qquad \frac{\mathrm{d}\hat{N}_i(t)}{\mathrm{d}t} = \hat{\mathcal{B}}_i(t) - \hat{\mathcal{D}}_i(t), \text{ with initial conditions,} \quad \hat{N}_i(0) = \hat{N}_i^0 \geq 0,$$

for all $i = 1, 2, \ldots, I$ and $\hat{N}_i(t)$ be the solution of (2.14). Here, the modified birth term is defined as

$$(2.15) \qquad \hat{\mathcal{B}}_i(t) = \begin{cases} b_i^{(2)} + b_{i+1}^{(3)}, & i = 1, \\ b_{i-1}^{(1)} + b_i^{(2)} + b_{i+1}^{(3)}, & i = 2, 3, \ldots, I-1, \\ b_{i-1}^{(1)} + b_i^{(2)}, & i = I, \end{cases}$$

where

$$b_{i-1}^{(1)} := \lambda_i^-(\bar{v}_{i-1}) H(\bar{v}_{i-1} - x_{i-1}) \hat{B}_{i-1}(t), \quad b_i^{(2)} := \lambda_i^-(\bar{v}_i) H(x_i - \bar{v}_i) \hat{B}_i(t) + \lambda_i^+(\bar{v}_i) H(\bar{v}_i - x_i) \hat{B}_i(t),$$

$$b_{i+1}^{(3)} := \lambda_i^+(\bar{v}_{i+1}) H(x_{i+1} - \bar{v}_{i+1}) \hat{B}_{i+1}(t) \quad \text{and} \quad H(x) = \begin{cases} 1, & x > 0, \\ 1/2, & x = 0, \\ 0, & x < 0, \end{cases} \text{ is the Heaviside function.}$$

The death term is defined by

$$(2.16) \qquad \hat{\mathcal{D}}_i(t) = \sum_{j=1}^{I} \mathcal{K}(x_i, x_j) \hat{N}_i(t) \hat{N}_j(t).$$

Throughout the study we take the following assumptions as:
(i) The collisional kernel satisfies $\mathcal{K} \in \mathcal{C}(\mathbb{R}_+^2)$. Therefore, for all $y, z \in [x_{\min}, x_{\max}]$, there exists a constant C depending on $x_{\max}$ only such that

$$(2.17) \qquad \sup_{(y,z) \in [x_{\min}, x_{\max}]^2} |\mathcal{K}(y, z)| \leq C(x_{\max}).$$

Note that using the inequality (2.17) together with equation (1.6) in the discrete equation (2.14) the time evolution of the discrete zeroth moment is defined as

$$(2.18) \qquad \frac{\mathrm{d}\hat{\mathcal{M}}_0(t)}{\mathrm{d}t} \leq [\bar{\zeta} - 1] C(x_{\max}) \hat{\mathcal{M}}_0^2(t).$$

Thus, the time evolution of the discrete zeroth moment or the total number of particles is bounded on a finite time interval $[0, T]$. So, there exists a constant $\beta(T)$ such that

$$(2.19) \qquad \hat{\mathcal{M}}_0(t) \leq \beta(T), \quad \text{for all} \quad t \in [0, T].$$

Proposition 2.1. *The discrete scheme* (2.14)-(2.16) *satisfies the volume conservation law and consistent with the temporal evolution of zeroth moment.*

Proof. Multiplying x_i to the equation (2.14) and summing over i, we obtain

$$\frac{\mathrm{d}}{\mathrm{d}t}\sum_{i=1}^{I}x_i\hat{N}_i(t) = \sum_{i=1}^{I}x_i\hat{B}_{i-1}(t)\lambda_i^-(\bar{v}_{i-1})H(\bar{v}_{i-1}-x_{i-1}) + \sum_{i=1}^{I}x_i\hat{B}_i(t)\lambda_i^-(\bar{v}_i)H(x_i-\bar{v}_i)$$

$$+ \sum_{i=1}^{I}x_i\hat{B}_i(t)\lambda_i^+(\bar{v}_i)H(\bar{v}_i-x_i) + \sum_{i=1}^{I}x_i\hat{B}_{i+1}(t)\lambda_i^+(\bar{v}_{i+1})H(x_{i+1}-\bar{v}_{i+1})$$

$$(2.20) \qquad - \sum_{i=1}^{I}\sum_{j=1}^{I}x_i\mathcal{K}(x_i,x_j)\hat{N}_i(t)\hat{N}_j(t).$$

Using the definition of $\lambda_i^{\pm}$ (2.13) and $H(x)$ in equation (2.20), we obtain

$$(2.21) \qquad \frac{\mathrm{d}}{\mathrm{d}t}\sum_{i=1}^{I}x_i\hat{N}_i(t) = \sum_{i=1}^{I}\bar{v}_i\hat{B}_i(t) - \sum_{i=1}^{I}\sum_{j=1}^{I}x_i\mathcal{K}(x_i,x_j)\hat{N}_i(t)\hat{N}_j(t)$$

$$= \sum_{i=1}^{I}\sum_{k=1}^{I}\sum_{j=i}^{I}\mathcal{K}(x_j,x_k)\hat{N}_j(t)\hat{N}_k(t)\int_{x_{i-1/2}}^{p_j^i} x\beta(x|x_j;x_k)\mathrm{d}x$$

$$(2.22) \qquad - \sum_{i=1}^{I}\sum_{j=1}^{I}x_i\mathcal{K}(x_i,x_j)\hat{N}_i(t)\hat{N}_j(t).$$

(see Appendix A to derive equation (2.21) for detailed calculation). Changing order of summations of the above equation (2.22), we get

$$\frac{\mathrm{d}}{\mathrm{d}t}\sum_{i=1}^{I}x_i\hat{N}_i(t) = \sum_{k=1}^{I}\sum_{j=1}^{I}\mathcal{K}(x_j,x_k)\hat{N}_j(t)\hat{N}_k(t)\sum_{i=1}^{j}\int_{x_{i-1/2}}^{p_i^j} x\beta(x|x_j;x_k)\mathrm{d}x$$

$$(2.23) \qquad - \sum_{i=1}^{I}\sum_{j=1}^{I}x_i\mathcal{K}(x_i,x_j)\hat{N}_i(t)\hat{N}_j(t).$$

Using volume preserving property (1.4) in equation (2.23) and simplifying calculation, it yields

$$\frac{\mathrm{d}}{\mathrm{d}t}\sum_{i=1}^{I}x_i\hat{N}_i(t) = \sum_{k=1}^{I}\sum_{j=1}^{I}x_j\mathcal{K}(x_j,x_k)\hat{N}_j(t)\hat{N}_k(t) - \sum_{i=1}^{I}\sum_{j=1}^{I}x_i\mathcal{K}(x_i,x_j)\hat{N}_i(t)\hat{N}_j(t) = 0,$$

that is $\hat{\mathcal{M}}_1(t) = \hat{\mathcal{M}}_1(0)$ for all $t \geq 0$, which is the volume conservation law.

The time evolution of the discrete zeroth moment is calculated by taking summation over i on discrete equation (2.14) and calculating in similar way as volume conservation and using property (1.5)

$$\frac{\mathrm{d}}{\mathrm{d}t}\sum_{i=1}^{I}\hat{N}_i(t) = \sum_{k=1}^{I}\sum_{j=i}^{I}\mathcal{K}(x_j,x_k)\hat{N}_j(t)\hat{N}_k(t)\sum_{i=1}^{j}\int_{x_{i-1/2}}^{p_j^i}\beta(x|x_j;x_k)\mathrm{d}x - \sum_{i=1}^{I}\sum_{j=1}^{I}\mathcal{K}(x_i,x_j)\hat{N}_i(t)\hat{N}_j(t)$$

$$= \sum_{k=1}^{I}\sum_{j=1}^{I}\mathcal{K}(x_j,x_k)\hat{N}_j(t)\hat{N}_k(t)\zeta(x_j,x_k) - \sum_{i=1}^{I}\sum_{j=1}^{I}\mathcal{K}(x_i,x_j)\hat{N}_i(t)\hat{N}_j(t)$$

$$= \sum_{k=1}^{I}\sum_{j=1}^{I}\mathcal{K}(x_j,x_k)\hat{N}_j(t)\hat{N}_k(t)\left[\zeta(x_j,x_k)-1\right].$$

This is equivalent with the time evolution of discrete zeroth moment (2.8). $\square$

Here, we are a position to introduce the semi-discrete system in a vector form described by reformulation(2.14) as follows: $\hat{\boldsymbol{N}} = \left\{\hat{N}_1, \hat{N}_2, \ldots, \hat{N}_I\right\} \in \mathbb{R}^I$ is the numerical solution of the following semi-discrete system

$$(2.24) \qquad \frac{\mathrm{d}\hat{\boldsymbol{N}}}{\mathrm{d}t} = \hat{\boldsymbol{B}}(\hat{\boldsymbol{N}}) - \hat{\boldsymbol{D}}(\hat{\boldsymbol{N}}) := \hat{\boldsymbol{J}}(\hat{\boldsymbol{N}}) \quad \text{with} \quad \hat{\boldsymbol{N}}(0) = \hat{\boldsymbol{N}}^0 \geq 0,$$

where i^{th} components of $\hat{\boldsymbol{\mathcal{B}}}, \hat{\boldsymbol{\mathcal{D}}} \in \mathbb{R}^I$ are defined by $\hat{\mathcal{B}}_i$ (2.15) and $\hat{\mathcal{D}}_i$ (2.16) and also the numerical flux $\hat{\boldsymbol{J}} = \left\{ \hat{J}_1, \hat{J}_2, \ldots, \hat{J}_I \right\} \in \mathbb{R}^I$ is a non negative vector whose i^{th} component is given by $\hat{J}_i = \hat{\mathcal{B}}_i - \hat{\mathcal{D}}_i$.

3. Stability and consistency

3.1. **Preliminary definitions and theorems.** Here, we assume the space $X = \mathbb{R}^I$ equipped with the discrete L^1-norm defined by

$$(3.1) \qquad ||\hat{\boldsymbol{N}}(t)|| = \sum_{i=1}^{I} |\hat{N}_i(t)|, \quad \text{for all } 0 \le t \le T.$$

Definition 3.1. (Spatial truncation error). The discretization residue obtained due to the substitution of the exact solution in the discrete scheme (2.24) is called truncation error and is mathematically calculated as

$$(3.2) \qquad \sigma(t) = \frac{\mathrm{d}\boldsymbol{N}(t)}{\mathrm{d}t} - \frac{\mathrm{d}\hat{\boldsymbol{N}}(t)}{\mathrm{d}t}, \quad \text{for all } 0 \le t \le T$$

where $\sigma = \{\sigma_1, \sigma_2, \ldots, \sigma_I\}$ is a vector whose i^{th} component is given by $\sigma_i(t) = \dfrac{\mathrm{d}N_i(t)}{\mathrm{d}t} - \dfrac{\mathrm{d}\hat{N}_i(t)}{\mathrm{d}t}$.

Definition 3.2. (Global discretization error). A numerical method is called the pth order convergent if for $\Delta x \to 0$

$$(3.3) \qquad ||\boldsymbol{N}(t) - \hat{\boldsymbol{N}}(t)|| = \mathcal{O}(\Delta x^p) \quad \text{for all } 0 \le t \le T.$$

Definition 3.3. (Lipschitz condition). A mapping $\hat{J}$ which follows

$$(3.4) \qquad ||\hat{\boldsymbol{J}}(\boldsymbol{g}) - \hat{\boldsymbol{J}}(\boldsymbol{h})|| \le \gamma ||\boldsymbol{g} - \boldsymbol{h}|| \quad \text{for all } \boldsymbol{g}, \boldsymbol{h} \in \mathbb{R}^I,$$

is said to be satisfy the Lipschitz condition with $\gamma < \infty$ as Lipschitz constant.

Definition 3.4. (Nonnegativity). The system of ODEs in $\mathbb{R}^I$ defined by (2.24) is called nonnegative or nonnegativity preserving if

$$(3.5) \qquad \hat{\boldsymbol{N}}(0) \ge 0 \text{ implies } \hat{\boldsymbol{N}}(t) \ge 0 \quad \text{for all } \quad 0 \le t \le T.$$

Definition 3.5. (Consistency). A numerical scheme is called p^{th} order consistent if for $\Delta x \to 0$

$$(3.6) \qquad ||\sigma(t)|| = \mathcal{O}(\Delta x^p) \quad \text{uniformly for all } 0 \le t \le T.$$

Proposition 3.1. *Let $\hat{\boldsymbol{J}} \in \mathbb{R}^I$ be the numerical flux defined by the equation (2.24) in the new scheme VAM. Then $\hat{\boldsymbol{J}}$ satisfies the Lipschitz condition.*

Proof. Let $\hat{\boldsymbol{M}}, \hat{\boldsymbol{N}} \in \mathbb{R}^I$ be two solutions satisfying the discrete system (2.24).

$$
\begin{aligned}
||\hat{\boldsymbol{\mathcal{B}}}(\hat{\boldsymbol{M}}) - \hat{\boldsymbol{\mathcal{B}}}(\hat{\boldsymbol{N}})|| = \sum_{i=1}^{I} \Bigg| & \lambda_i^-(\bar{v}_{i-1}) H(\bar{v}_{i-1} - x_{i-1}) \left(\hat{B}_{i-1}(\hat{\boldsymbol{M}}) - \hat{B}_{i-1}(\hat{\boldsymbol{N}}) \right) \\
& + \lambda_i^-(\bar{v}_i) H(x_i - \bar{v}_i) \left(\hat{B}_i(\hat{\boldsymbol{M}}) - \hat{B}_i(\hat{\boldsymbol{N}}) \right) + \lambda_i^+(\bar{v}_i) H(\bar{v}_i - x_i) \left(\hat{B}_i(\hat{\boldsymbol{M}}) - \hat{B}_i(\hat{\boldsymbol{N}}) \right) \\
& + \lambda_i^+(\bar{v}_{i+1}) H(x_{i+1} - \bar{v}_{i+1}) \left(\hat{B}_{i+1}(\hat{\boldsymbol{M}}) - \hat{B}_{i+1}(\hat{\boldsymbol{N}}) \right) \Bigg| \\
\le & \sum_{i=1}^{I} \lambda_i^-(\bar{v}_{i-1}) H(\bar{v}_{i-1} - x_{i-1}) \left| \hat{B}_{i-1}(\hat{\boldsymbol{M}}) - \hat{B}_{i-1}(\hat{\boldsymbol{N}}) \right| \\
& + \sum_{i=1}^{I} \lambda_i^-(\bar{v}_i) H(x_i - \bar{v}_i) \left| \hat{B}_i(\hat{\boldsymbol{M}}) - \hat{B}_i(\hat{\boldsymbol{N}}) \right| \\
& + \sum_{i=1}^{I} \lambda_i^+(\bar{v}_i) H(\bar{v}_i - x_i) \left| \hat{B}_i(\hat{\boldsymbol{M}}) - \hat{B}_i(\hat{\boldsymbol{N}}) \right|
\end{aligned}
$$

$$(3.7) \qquad + \sum_{i=1}^{I} \lambda_i^+(\bar{v}_{i+1}) H(x_{i+1} - \bar{v}_{i+1}) \left| \hat{B}_{i+1}(\hat{M}) - \hat{B}_{i+1}(\hat{N}) \right|.$$

By the definitions of $\lambda_i^{\pm}(x)$ and $H(x)$, we have

$$0 \leq \lambda_i^{\pm}(x) H(x) \leq 1.$$

Thereby, estimation (3.7) can be written as

$$||\hat{\boldsymbol{\mathcal{B}}}(\hat{M}) - \hat{\boldsymbol{\mathcal{B}}}(\hat{N})|| \leq \sum_{i=1}^{I} \left| \hat{B}_{i-1}(\hat{M}) - \hat{B}_{i-1}(\hat{N}) \right| + \sum_{i=1}^{I} \left| \hat{B}_i(\hat{M}) - \hat{B}_i(\hat{N}) \right|$$

$$(3.8) \qquad + \sum_{i=1}^{I} \left| \hat{B}_{i+1}(\hat{M}) - \hat{B}_{i+1}(\hat{N}) \right|.$$

Using definition of $\hat{\beta}_i$ and property (1.5), bounds of $\mathcal{K}$ (2.17) and boundedness of the discrete zeroth moment $\hat{\mathcal{M}}_0$ (2.19), we deduce that

$$\left| \hat{\mathcal{B}}_i(\hat{M}) - \hat{\mathcal{B}}_i(\hat{N}) \right| = \sum_{i=1}^{I} \sum_{k=1}^{I} \sum_{j=i}^{I} \mathcal{K}(x_j, x_k) \left| \hat{M}_j \hat{M}_k - \hat{N}_j \hat{N}_k \right| \int_{x_{i-1/2}}^{p_j^i} \beta(x|x_j, x_k) \mathrm{d}x$$

$$\leq \bar{\zeta} C(x_{\max}) \sum_{k=1}^{I} \sum_{j=1}^{I} \frac{1}{2} \left| \left(\hat{M}_j + \hat{N}_j \right) \left(\hat{M}_k - \hat{N}_k \right) + \left(\hat{M}_j - \hat{N}_j \right) \left(\hat{M}_K + \hat{N}_k \right) \right|$$

$$\leq \frac{\bar{\zeta} C(x_{\max})}{2} \times 2 \left(\sum_{j=1}^{I} \left| \hat{M}_j + \hat{N}_j \right| \right) \left(\sum_{k=1}^{I} \left| \hat{M}_k - \hat{N}_k \right| \right)$$

$$(3.9) \qquad \leq 2 \bar{\zeta} C(x_{\max}) \beta(T) ||\hat{M} - \hat{N}||.$$

In similar way, for death term we obtain

$$(3.10) \qquad \qquad ||\hat{\boldsymbol{\mathcal{D}}}(\hat{M}) - \hat{\boldsymbol{\mathcal{D}}}(\hat{N})|| \leq 2 C(x_{\max}) \beta(T) ||\hat{M} - \hat{N}||.$$

Thereby birth term from (3.9) and death term from (3.10), combinedly we may write

$$\left\| \left(\hat{\boldsymbol{\mathcal{B}}}(\hat{M}) - \hat{\boldsymbol{\mathcal{D}}}(\hat{M}) \right) - \left(\hat{\boldsymbol{\mathcal{B}}}(\hat{N}) - \hat{\boldsymbol{\mathcal{D}}}(\hat{N}) \right) \right\| \leq ||\hat{\boldsymbol{\mathcal{B}}}(\hat{M}) - \hat{\boldsymbol{\mathcal{B}}}(\hat{N})|| + ||\hat{\boldsymbol{\mathcal{D}}}(\hat{M}) - \hat{\boldsymbol{\mathcal{D}}}(\hat{N})||$$

$$\leq 2(\bar{\zeta} + 1) C(x_{\max}) \beta(T) ||\hat{M} - \hat{N}||$$

$$\leq \eta ||\hat{M} - \hat{N}||,$$

where $\eta := 2(\bar{\zeta} + 1) C(x_{\max}) \beta(T) < \infty$ is a constant, independent of the grids.
Finally, we can write

$$||\hat{\boldsymbol{J}}(\hat{M}) - \hat{\boldsymbol{J}}(\hat{N})|| \leq \eta ||\hat{M} - \hat{N}||,$$

which implies that the $\hat{\boldsymbol{J}}$ satisfies the Lipschitz condition irrespective of the grids. $\qquad \square$

3.2. Nonnegativity of the solution.

Theorem 3.1. *Let $\hat{\boldsymbol{J}}(\hat{N})$ be a continuous mapping satisfying Lipschitz condition with respect to $\hat{N}$. Then the semi-discrete system (2.24) is nonnegative, if and only if for any vector $\hat{N} \in \mathbb{R}^I$ satisfying*

$$(3.11) \qquad \qquad \hat{N} \geq 0, \quad with \quad \hat{N}_i = 0 \text{ implies } \hat{\boldsymbol{J}}(\hat{N}) \geq 0,$$

which proves that the solution by the new scheme VAM (2.14) is nonnegative.

Proof. Assume that the semi-discrete system (2.24) is nonnegative. Let $\hat{N}$ be the solution of the system (2.24) with initial conditions $\hat{N}(0) \geq 0$. By definition 3.4 of the ODE system, we have $\hat{N} \geq 0$. Now, $\hat{N} \geq 0$ with $\hat{N}_i = 0$ implies $\hat{\mathcal{B}}_i(\hat{N}) \geq 0$ and $\hat{\mathcal{D}}_i(\hat{N}) = 0$ for all $i \in \{1, 2, \ldots, I\}$. So, $\hat{N} \geq 0$ with $\hat{N}_i = 0$ deduces that $\hat{J}_i(\hat{N}) \geq 0$ for all $i = 1, 2, \ldots, I$ which implies $\hat{\boldsymbol{J}}(\hat{N}) \geq 0$.
Conversely, we have the criteria

$$\hat{N} \geq 0, \quad with \quad \hat{N}_i = 0 \text{ implies } \hat{\boldsymbol{J}}(\hat{N}) \geq 0.$$

The above expression implies $\dfrac{\mathrm{d}\hat{N}_i}{\mathrm{d}t} \geq 0$. To prove the nonnegativity, we will use the Lipschitz condition on $\hat{\boldsymbol{J}}$. Since the solution $\hat{\boldsymbol{N}}$ can not cross the hyperplane $\mathcal{H}_i = \left\{ \hat{\boldsymbol{N}} \in \mathbb{R}^I : \hat{N}_i = 0 \right\}$ so there exists sufficiently small $\varepsilon > 0$ such that

$$\hat{\boldsymbol{N}} \geq 0, \quad \text{with} \quad \hat{N}_i = 0 \ \text{ implies } \ \frac{\mathrm{d}\hat{N}_i}{\mathrm{d}t} \geq \varepsilon > 0.$$

This will satisfy the the perturbed ODE system with

$$\tilde{J}_i = \hat{J}_i + \varepsilon, \quad \text{for all} \quad i = 1, 2, \ldots, I.$$

By the Lipschitz condition of $\hat{\boldsymbol{J}}$ and using the standard stability argument for ODEs, if $\varepsilon \to 0$, the solution of the unperturbed system with given initial condition will be approximated with exact solution of the perturbed system. This above argument and the criteria (3.11), we can write that the system (2.24) is nonnegative.

For the second part, we have already proved that the system of ODEs (2.24) is nonnegative in the first part. This directly implies that the solution by the new scheme VAM is nonnegative. $\qquad\square$

3.3. Consistency.

To find the error estimations of approximated birth term, death term and total volume flux, we need to integrate the birth term and death term of equation (2.1) with total volume flux over Λ_i and hence define

$$(3.12\mathrm{a}) \qquad B_i(t) := \int_{x_{i-1/2}}^{x_{i+1/2}} \int_0^{x_{\max}} \int_x^{x_{\max}} \beta(x|y;z)\mathcal{K}(y,z)n(y,t)n(z,t)\mathrm{d}y\mathrm{d}z\mathrm{d}x,$$

$$(3.12\mathrm{b}) \qquad D_i(t) := \int_{x_{i-1/2}}^{x_{i+1/2}} \int_0^{x_{\max}} \mathcal{K}(x,y)n(x,t)n(y,t)\mathrm{d}y\mathrm{d}x,$$

$$(3.12\mathrm{c}) \qquad V_i(t) := \int_{x_{i-1/2}}^{x_{i+1/2}} \int_0^{x_{\max}} \int_x^{x_{\max}} x\beta(x|y;z)\mathcal{K}(y,z)n(y,t)n(z,t)\mathrm{d}y\mathrm{d}z\mathrm{d}x.$$

Lemma 3.1. *Let B_i, D_i, V_i, $\hat{B}_i$, $\hat{D}_i$, $\hat{V}_i$ are defined by the equations (3.12), (2.5) and (2.10) respectively. Then we have the following error estimates:*

$$(3.13\mathrm{a}) \ (i) \quad B_i = \hat{B}_i + \mathcal{O}(\Delta x_i^3),$$

$$(3.13\mathrm{b}) \ (ii) \quad D_i = \hat{D}_i + \mathcal{O}(\Delta x_i^3),$$

$$(3.13\mathrm{c}) \ (iii) \quad V_i = \hat{V}_i + \mathcal{O}(\Delta x_i^3).$$

Proof. Considering $B_i(t)$ and the fact that z is independent of x and y, so we change the order of integration and rearrange the integrals in simplified discretized form to get

$$B_i(t) = \int_0^{x_{I+1/2}} \int_{x_{i-1/2}}^{x_{i+1/2}} \int_{x_{i-1/2}}^y \beta(x|y;z)\mathcal{K}(y,z)n(y,t)n(z,t)\mathrm{d}x\mathrm{d}y\mathrm{d}z$$
$$+ \int_0^{x_{I+1/2}} \int_{x_{i+1/2}}^{x_{I+1/2}} \int_{x_{i-1/2}}^{x_{i+1/2}} \beta(x|y;z)\mathcal{K}(y,z)n(y,t)n(z,t)\mathrm{d}x\mathrm{d}y\mathrm{d}z.$$

Applying the midpoint quadrature rule for first two integrals of above equation, we get

$$B_i(t) = \sum_{k=1}^I \mathcal{K}(x_i,x_k)N_i(t)N_k(t) \int_{x_{i-1/2}}^{x_i} \beta(x|x_i;x_k)\mathrm{d}x + \mathcal{O}(\Delta x_i^3)$$
$$+ \sum_{k=1}^I \sum_{j=i+1}^I \mathcal{K}(x_j,x_k)N_j(t)N_k(t) \int_{x_{i-1/2}}^{x_{i+1/2}} \beta(x|x_j;x_k)\mathrm{d}x + \mathcal{O}(\Delta x_i^3)$$
$$= \sum_{k=1}^I \sum_{j=i}^I \mathcal{K}(x_j,x_k)N_j(t)N_k(t) \int_{x_{i-1/2}}^{p_j^i} \beta(x|x_j;x_k)\mathrm{d}x + \mathcal{O}(\Delta x_i^3)$$

$$= \sum_{k=1}^{I} \sum_{j=i}^{I} \beta_{i,j}^{k} \mathcal{K}(x_j, x_k) N_j(t) N_k(t) + \mathcal{O}(\Delta x_i^3).$$

Therefore, we have

(3.14)
$$B_i(t) = \hat{B}_i(t) + \mathcal{O}(\Delta x_i^3).$$

Similarly, the death term (3.12) can be written as

(3.15)
$$D_i(t) = \sum_{j=1}^{I} \mathcal{K}(x_i, x_j) N_i(t) N_j(t) + \mathcal{O}(\Delta x_i^3) = \hat{D}_i(t) + \mathcal{O}(\Delta x_i^3),$$

and the volume flux is written as

$$V_i(t) = \sum_{k=1}^{I} \sum_{j=i}^{I} \mathcal{K}(x_j, x_k) N_j(t) N_k(t) \int_{x_{i-1/2}}^{p_j^i} x \beta(x|x_j, x_k) \mathrm{d}x + \mathcal{O}(\Delta x_i^3) = \hat{V}_i(t) + \mathcal{O}(\Delta x_i^3).$$

$\square$

We now recall the discrete scheme VAM and simplify each term in the scheme separately. By using the definition of λ_i and $\hat{\mathcal{B}}_i(t)$, we can write the following term as

(3.16)
$$\lambda_i^-(\bar{v}_{i-1}) \hat{B}_{i-1}(t) = \frac{\bar{v}_{i-1} - x_{i-1}}{x_i - x_{i-1}} \hat{B}_{i-1}(t) = \frac{2}{\Delta x_i + \Delta x_{i-1}} \left[\bar{v}_{i-1} \hat{B}_{i-1}(t) - x_{i-1} \hat{B}_{i-1}(t) \right].$$

Substituting the values of $\hat{B}_{i-1}(t)$ (2.5) and $\bar{v}_{i-1}$ (2.11) in equation (3.16), we obtain

$$\lambda_i^-(\bar{v}_{i-1}) \hat{B}_{i-1}(t) = \frac{2}{\Delta x_i + \Delta x_{i-1}} \left[\sum_{k=1}^{I} \sum_{j=i-1}^{I} \mathcal{K}(x_j, x_k) \hat{N}_j(t) \hat{N}_k(t) \int_{x_{i-3/2}}^{p_j^{i-1}} x \beta(x|x_j; x_k) \mathrm{d}x \right.$$

$$- x_{i-1} \sum_{k=1}^{I} \sum_{j=i-1}^{I} \mathcal{K}(x_j, x_k) \hat{N}_j(t) \hat{N}_k(t) \int_{x_{i-3/2}}^{p_j^{i-1}} \beta(x|x_j; x_k) \mathrm{d}x \right]$$

$$= \frac{2}{\Delta x_i + \Delta x_{i-1}} \left[\sum_{k=1}^{I} \sum_{j=i-1}^{I} \mathcal{K}(x_j, x_k) \hat{N}_j(t) \hat{N}_k(t) \int_{x_{i-3/2}}^{p_j^{i-1}} (x - x_{i-1}) \beta(x|x_j; x_k) \mathrm{d}x \right]$$

$$= \frac{2}{\Delta x_i + \Delta x_{i-1}} \left[\sum_{k=1}^{I} \mathcal{K}(x_{i-1}, x_k) \hat{N}_{i-1}(t) \hat{N}_k(t) \int_{x_{i-3/2}}^{x_{i-1}} (x - x_{i-1}) \beta(x|x_{i-1}; x_k) \mathrm{d}x \right.$$

(3.17)
$$\left. + \sum_{k=1}^{I} \sum_{j=i}^{I} \mathcal{K}(x_j, x_k) \hat{N}_j(t) \hat{N}_k(t) \int_{x_{i-3/2}}^{x_{i-1/2}} (x - x_{i-1}) \beta(x|x_j; x_k) \mathrm{d}x \right].$$

Assume sufficient smoothness on β with respect to x and consider $g(x) := (x - x_{i-1}) \beta(x|x_{i-1}; x_k)$. Applying Taylor series expansions about $x = x_{i-1}$ of function $g(x)$ having nonzero derivatives upto second order, we obtain

(3.18)
$$g(x) = g(x_{i-1}) + (x - x_{i-1}) g'(x_{i-1}) + \mathcal{O}(\Delta x_i^2) = (x - x_{i-1}) \beta(x_{i-1}|x_{i-1}; x_k) + \mathcal{O}(\Delta x_i^2).$$

By applying the similar argument on $h(x) := (x - x_{i-1}) \beta(x|x_j; x_k)$, we obtain

(3.19)
$$h(x) = (x - x_{i-1}) \beta(x_{i-1}|x_j; x_k) + (x - x_{i-1})^2 \beta_x(x_{i-1}|x_j; x_k) + \mathcal{O}(\Delta x_i^3).$$

Now substituting the estimates of g and h in (3.17) and using (2.3), it yields

$$\lambda_i^-(\bar{v}_{i-1}) \hat{B}_{i-1}(t) = \frac{2}{\Delta x_i + \Delta x_{i-1}} \left[\sum_{k=1}^{I} \mathcal{K}(x_{i-1}, x_k) \hat{N}_{i-1}(t) \hat{N}_k(t) \int_{x_{i-3/2}}^{x_{i-1}} g(x) \mathrm{d}x \right.$$

$$\left. + \sum_{k=1}^{I} \sum_{j=i}^{I} \mathcal{K}(x_j, x_k) \hat{N}_j(t) \hat{N}_k(t) \int_{x_{i-3/2}}^{x_{i-1/2}} h(x) \mathrm{d}x \right] + \mathcal{O}(\Delta x_i^3)$$

$$= \frac{2}{\Delta x_i + \Delta x_{i-1}} \left(-\frac{1}{8} \sum_{k=1}^{I} \beta(x_{i-1}|x_{i-1}; x_k) \mathcal{K}(x_{i-1}, x_k) \hat{N}_{i-1}(t) \hat{N}_k(t) \Delta x_{i-1}^2 \right.$$

$$+ \frac{1}{12} \sum_{k=1}^{I} \sum_{j=i}^{I} \beta_x(x_{i-1}|x_j;x_k)\mathcal{K}(x_j,x_k)\hat{N}_j(t)\hat{N}_k(t)\Delta x_{i-1}^3 \bigg) + \mathcal{O}(\Delta x_i^3).$$

Let $\bar{h}(x_{i-1}) = \beta(x_{i-1}|x_{i-1};x_k)\mathcal{K}(x_{i-1},x_k)N_{i-1}(t)$ and $\bar{g}(x_{i-1}) = \beta_x(x_{i-1}|x_j;x_k)$ from the above equation. Applying forwarded difference on $\bar{h}$ and $\bar{g}$ about x_i in the above equation, we obtain

$$\lambda_i^-(\bar{v}_{i-1})\hat{B}_{i-1}(t) = - \frac{\Delta x_{i-1}^2}{\Delta x_i + \Delta x_{i-1}} \times \frac{1}{4} \sum_{k=1}^{I} \beta(x_i|x_i;x_k)\mathcal{K}(x_i,x_k)\hat{N}_i(t)\hat{N}_k(t)$$

$$+ \frac{\Delta x_{i-1}^3}{\Delta x_i + \Delta x_{i-1}} \times \frac{1}{6} \sum_{k=1}^{I} \sum_{j=i}^{I} \beta_x(x_i|x_j;x_k)\mathcal{K}(x_j,x_k)\hat{N}_j(t)\hat{N}_k(t) + \mathcal{O}(\Delta x_i^3).$$

Similarly, we can obtain the second term as

$$\lambda_i^+(\bar{v}_i)\hat{B}_i(t) = \frac{\bar{v}_i - x_{i+1}}{x_i - x_{i+1}}\hat{B}_i(t) = \left(1 - \frac{\bar{v}_i - x_i}{x_{i+1} - x_i}\right)\hat{B}_i(t)$$

$$= \hat{B}_i(t) + \frac{\Delta x_i^2}{\Delta x_i + \Delta x_{i+1}} \times \frac{1}{4} \sum_{k=1}^{I} \beta(x_i|x_i;x_k)\mathcal{K}(x_i,x_k)\hat{N}_i(t)\hat{N}_k(t)$$

$$- \frac{\Delta x_i^3}{\Delta x_i + \Delta x_{i+1}} \times \frac{1}{6} \sum_{k=1}^{I} \sum_{j=i+1}^{I} \beta_x(x_i|x_j;x_k)\mathcal{K}(x_j,x_k)\hat{N}_j(t)\hat{N}_k(t) + \mathcal{O}(\Delta x_i^3).$$

As in previous way, the third term is

$$\lambda_i^-(\bar{v}_i)\hat{B}_i(t) = \frac{\bar{v}_i - x_{i-1}}{x_i - x_{i-1}}\hat{B}_i(t) = \left(1 + \frac{\bar{v}_i - x_i}{x_i - x_{i-1}}\right)\hat{B}_i(t)$$

$$= \frac{\bar{v}_i - x_{i+1}}{x_i - x_{i+1}}\hat{B}_i(t) = \left(1 - \frac{\bar{v}_i - x_i}{x_{i+1} - x_i}\right)\hat{B}_i(t)$$

$$= \hat{B}_i(t) - \frac{\Delta x_i^2}{\Delta x_i + \Delta x_{i+1}} \times \frac{1}{4} \sum_{k=1}^{I} \beta(x_i|x_i;x_k)\mathcal{K}(x_i,x_k)\hat{N}_i(t)\hat{N}_k(t)$$

$$+ \frac{\Delta x_i^3}{\Delta x_i + \Delta x_{i+1}} \times \frac{1}{6} \sum_{k=1}^{I} \sum_{j=i+1}^{I} \beta_x(x_i|x_j;x_k)\mathcal{K}(x_j,x_k)\hat{N}_j(t)\hat{N}_k(t) + \mathcal{O}(\Delta x_i^3).$$

The fourth term is given by

$$\lambda_i^-(\bar{v}_{i+1})\hat{B}_{i+1}(t) = \frac{\bar{v}_i - x_{i+1}}{x_i - x_{i+1}}\hat{B}_i(t)$$

$$= \frac{\Delta x_{i+1}^2}{\Delta x_i + \Delta x_{i+1}} \times \frac{1}{4} \sum_{k=1}^{I} \beta(x_i|x_i;x_k)\mathcal{K}(x_i,x_k)\hat{N}_i(t)\hat{N}_k(t)$$

$$- \frac{\Delta x_{i+1}^3}{\Delta x_i + \Delta x_{i+1}} \times \frac{1}{6} \sum_{k=1}^{I} \sum_{j=i+2}^{I} \beta_x(x_i|x_j;x_k)\mathcal{K}(x_j,x_k)\hat{N}_j(t)\hat{N}_k(t) + \mathcal{O}(\Delta x_i^3).$$

Without loss of generality, the summation appearing in all the above four expressions can be started from $(i+2)$ since the terms being omitted have 4th order accuracy. By error estimation Lemma 3.1 and setting $F(x|y;z) := \beta(x|y;z)\mathcal{K}(y,z)$ and $F_x(x|y;z) := \beta_x(x|y;z)\mathcal{K}(y,z)$, all four expressions rewritten in more simplified form as

$$\lambda_i^-(\bar{v}_{i-1})\hat{B}_{i-1}(t) = - \frac{\Delta x_{i-1}^2}{\Delta x_i + \Delta x_{i-1}} \times \frac{1}{4} \sum_{k=1}^{I} F(x_i|x_i;x_k)\hat{N}_i(t)\hat{N}_k(t)$$

$$+ \frac{\Delta x_{i-1}^3}{\Delta x_i + \Delta x_{i-1}} \times \frac{1}{6} \sum_{k=1}^{I} \sum_{j=i+2}^{I} F_x(x_i|x_j;x_k)\hat{N}_j(t)\hat{N}_k(t) + \mathcal{O}(\Delta x_i^3),$$

$$\lambda_i^+(\bar{v}_i)\hat{B}_i(t) = B_i(t) + \frac{\Delta x_i^2}{\Delta x_i + \Delta x_{i+1}} \times \frac{1}{4}\sum_{k=1}^{I}F(x_i|x_i;x_k)\hat{N}_i(t)\hat{N}_k(t)$$

$$- \frac{\Delta x_i^3}{\Delta x_i + \Delta x_{i+1}} \times \frac{1}{6}\sum_{k=1}^{I}\sum_{j=i+2}^{I}F_x(x_i|x_j;x_k)\hat{N}_j(t)\hat{N}_k(t) + \mathcal{O}(\Delta x_i^3),$$

$$\lambda_i^-(\bar{v}_i)\hat{B}_i(t) = B_i(t) - \frac{\Delta x_i^2}{\Delta x_i + \Delta x_{i-1}} \times \frac{1}{4}\sum_{k=1}^{I}F(x_i|x_i;x_k)\hat{N}_i(t)\hat{N}_k(t)$$

$$+ \frac{\Delta x_i^3}{\Delta x_i + \Delta x_{i-1}} \times \frac{1}{6}\sum_{k=1}^{I}\sum_{j=i+2}^{I}F_x(x_i|x_j;x_k)\hat{N}_j(t)\hat{N}_k(t) + \mathcal{O}(\Delta x_i^3)$$

and

$$\lambda_i^+(\bar{v}_{i+1})\hat{B}_{i+1}(t) = \frac{\Delta x_{i+1}^2}{\Delta x_i + \Delta x_{i+1}} \times \frac{1}{4}\sum_{k=1}^{I}F(x_i|x_i;x_k)\hat{N}_i(t)\hat{N}_k(t)$$

$$- \frac{\Delta x_{i+1}^3}{\Delta x_i + \Delta x_{i+1}} \times \frac{1}{6}\sum_{k=1}^{I}\sum_{j=i+2}^{I}F_x(x_i|x_j;x_k)\hat{N}_j(t)\hat{N}_k(t) + \mathcal{O}(\Delta x_i^3).$$

Depending on the position of volume average $\bar{v}_i$, there arise two cases arise: (see Figure 3)

Case I: Consider the particle average volume $\bar{v}_i$ in the right side of the pivot x_i that is
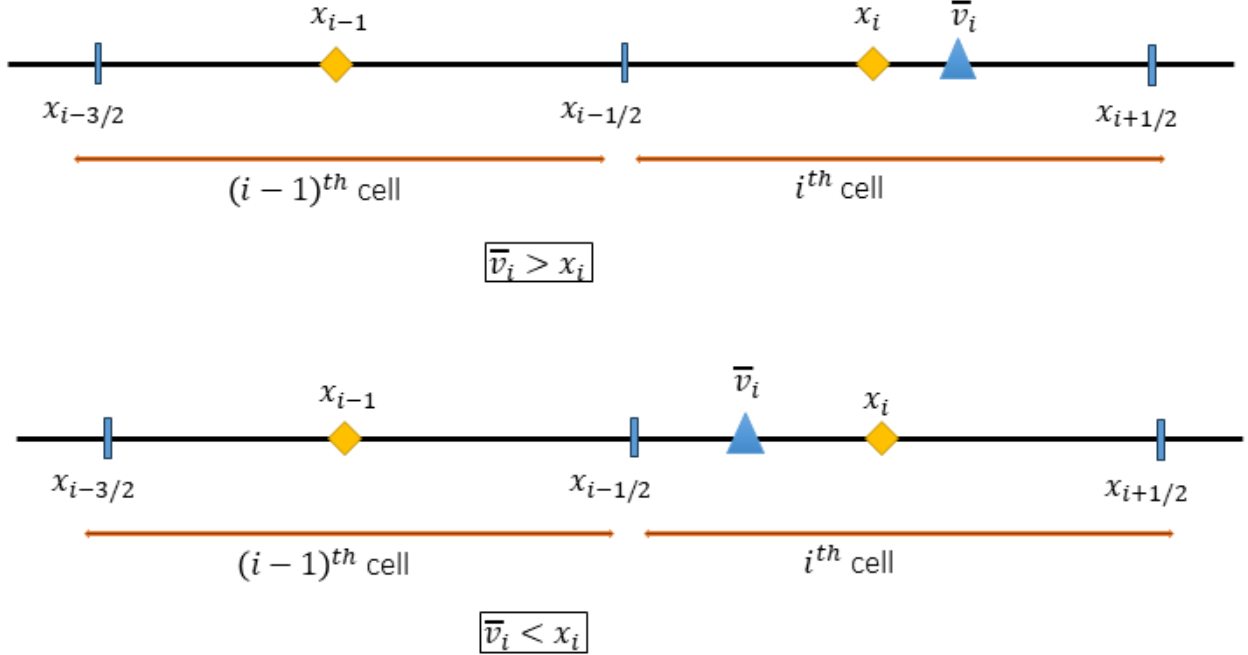

FIGURE 3. $\bar{v}_i > x_i$ and $\bar{v}_i < x_i$

$\bar{v}_{i-1} > x_{i-1}$, $\bar{v}_i > x_i$, $\bar{v}_{i+1} \geq x_{i+1}$. Then

$$\hat{\mathcal{B}}_i(t) = B_i(t) + \left(\frac{\Delta x_i^2}{\Delta x_i + \Delta x_{i+1}} - \frac{\Delta x_{i-1}^2}{\Delta x_i + \Delta x_{i-1}}\right) \times \frac{1}{4}\sum_{k=1}^{I}F(x_i|x_i;x_k)\hat{N}_i(t)\hat{N}_k(t)$$

$$- \left(\frac{\Delta x_i^3}{\Delta x_i + \Delta x_{i+1}} - \frac{\Delta x_{i-1}^3}{\Delta x_i + \Delta x_{i-1}}\right) \times \frac{1}{6}\sum_{k=1}^{I}\sum_{j=i+2}^{I}F_x(x_i|x_j;x_k)\hat{N}_j(t)\hat{N}_k(t) + \mathcal{O}(\Delta x_i^3).$$

Case II: Consider the particle average volume $\bar{v}_i$ in the left side of the pivot x_i that is $\bar{v}_{i-1} \le x_{i-1}$, $\bar{v}_i < x_i$, $\bar{v}_{i+1} < x_{i+1}$. Then

$$\hat{\mathcal{B}}_i(t) = B_i(t) + \left(\frac{\Delta x_{i+1}^2}{\Delta x_i + \Delta x_{i+1}} - \frac{\Delta x_i^2}{\Delta x_i + \Delta x_{i-1}} \right) \times \frac{1}{4} \sum_{k=1}^{I} F(x_i|x_i; x_k) \hat{N}_i(t) \hat{N}_k(t)$$
$$- \left(\frac{\Delta x_{i+1}^3}{\Delta x_i + \Delta x_{i+1}} - \frac{\Delta x_i^3}{\Delta x_i + \Delta x_{i-1}} \right) \times \frac{1}{6} \sum_{k=1}^{I} \sum_{j=i+2}^{I} F_x(x_i|x_j; x_k) \hat{N}_j(t) \hat{N}_k(t) + \mathcal{O}(\Delta x_i^3).$$

Remark 3.1. Consider breakage kernel $\beta(x|y; z) = \dfrac{12x}{y^2} \left(1 - \dfrac{x}{y} \right)$, therefore $F(x_i|x_i; x_k) = 0$. Then, **Case I** gives

$$\hat{\mathcal{B}}_i(t) = B_i(t) - \left(\frac{\Delta x_i^3}{\Delta x_i + \Delta x_{i+1}} - \frac{\Delta x_{i-1}^3}{\Delta x_i + \Delta x_{i-1}} \right) \times \frac{1}{6} \sum_{k=1}^{I} \sum_{j=i+2}^{I} F_x(x_i|x_j; x_k) \hat{N}_j(t) \hat{N}_k(t) + \mathcal{O}(\Delta x_i^3),$$

and **Case II** gives

$$\hat{\mathcal{B}}_i(t) = B_i(t) - \left(\frac{\Delta x_{i+1}^3}{\Delta x_i + \Delta x_{i+1}} - \frac{\Delta x_i^3}{\Delta x_i + \Delta x_{i-1}} \right) \times \frac{1}{6} \sum_{k=1}^{I} \sum_{j=i+2}^{I} F_x(x_i|x_j; x_k) \hat{N}_j(t) \hat{N}_k(t) + \mathcal{O}(\Delta x_i^3).$$

In order to investigate the consistency of the scheme, we will use these following results:

Lemma 3.2. *Let $0 < h \in \mathbb{R}^+$ and $B(x,t) \in \mathcal{C}^1(\mathbb{R}^+ \times \mathbb{R}^+)$, then for all $v \in \mathbb{R}^+$ we have*

$$\int_{v-h}^{v+h} (v-x)B(x,t)\mathrm{d}x \begin{cases} \ge 0, & \text{if } B(x,t) \text{ is monotonically decreasing for } x \in [v-h, v+h] \\ \le 0, & \text{if } B(x,t) \text{ is monotonically increasing for } x \in [v-h, v+h]. \end{cases}$$

Proof. Using Taylor's series, we have

$$(3.20) \qquad B(x,t) = B(v,t) + (v-x)B_x(\theta, t), \quad \text{for} \quad \theta \in [v-h, v+h].$$

Therefore, using (3.20) we have

$$(3.21) \qquad \int_{v-h}^{v+h} (v-x)B(x,t)\mathrm{d}x = \int_{v-h}^{v+h} (v-x)\left[B(v,t) + (x-v)B_x(\theta, t) \right] \mathrm{d}x, \quad \text{for} \quad \theta \in [v-h, v+h].$$

Since $B(x,t)$ is monotonically decreasing with respect to x for $x \in [v-h, v+h]$, we obtain $B_x(\theta, t) \le 0$. Moreover, evaluating the integrals in equation (3.21), we get

$$\int_{v-h}^{v+h} (v-x)B(x,t)\mathrm{d}x = -B(v,t)\int_{v-h}^{v+h} (x-v)\mathrm{d}x - \int_{v-h}^{v+h} (x-v)^2 B_x(\theta, t)\mathrm{d}x \ge 0.$$

Proceeding as first part, we can also prove the second part. $\qquad \square$

Lemma 3.3. *Assume that Σ be subset of $\mathbb{R}^+$. Let $\beta(x|y; z) : \mathcal{C}(\Sigma^3) \to \mathbb{R}^+$, $\mathcal{K}(y,z) : \mathcal{C}(\Sigma^2) \to \mathbb{R}^+$ and $n(x,t) : \mathcal{C}(\Sigma \times \mathbb{R}^+) \to \mathbb{R}^+$. If the birth rate function*

$$B(x,t) = \int_0^{x_{\max}} \int_x^{x_{\max}} \beta(x|y; z)\mathcal{K}(y,z)n(y,t)n(z,t)\mathrm{d}y\mathrm{d}z,$$

has finitely many oscillations (at the most a finite number of maxima and minima) in Σ at any time t, then the expression $x_i - \bar{v}_i$, $i = 1, 2, \ldots, I$ defined by using the equations (2.5) and (2.10)-(2.11)

$$x_i - \bar{v}_i = \frac{x_i \hat{B}_i - \hat{V}_i}{\hat{B}_i}, \quad \hat{B}_i > 0,$$

changes its sign at most finitely many times for Δx sufficiently small.

Proof. First assume that $B(x,t)$ has finitely many oscillations (at the most a finite number of maxima and minima) in domain Σ at any time t. So, domain Σ can be divided into m sub-domains $\Sigma_1, \Sigma_2, \ldots, \Sigma_m$ such that in each sub-domain Σ_k for $k = 1, 2, \ldots, m$ the function $B(x,t)$ is either monotonically decreasing or increasing. By Lemma 3.1, we obtain

$$
\begin{aligned}
x_i - \bar{v}_i &= \frac{x_i B_i - V_i + \mathcal{O}(\Delta x_i^3)}{\hat{B}_i} \\
&= \frac{\displaystyle\int_{x_{i-1/2}}^{x_{i+1/2}} \int_0^{x_{\max}} \int_x^{x_{\max}} (x_i - x)\beta(x|y;z)\mathcal{K}(y,z)n(y,t)n(z,t)\mathrm{d}y\mathrm{d}z\mathrm{d}x + \mathcal{O}(\Delta x_i^3)}{\hat{B}_i} \\
&= \frac{\displaystyle\int_{x_{i-1/2}}^{x_{i+1/2}} (x_i - x)B(x,t)\mathrm{d}x + \mathcal{O}(\Delta x_i^3)}{\hat{B}_i}.
\end{aligned}
$$

(3.22)

For sufficiently small Δx and Lemma 3.2, we get that $x_i - \bar{v}_i \geq 0$ in any one sub-domain of the sub-domains $\Sigma_1, \Sigma_2, \ldots, \Sigma_m$ where the function $B(x,t)$ is monotonically decreasing and $x_i - \bar{v}_i \leq 0$ in that sub-domain where the function $B(x,t)$ is monotonically increasing. Since we divide the domain into finite m sub-domains $\Sigma_1, \Sigma_2, \ldots, \Sigma_m$, the change of the sign of the function $x_i - \bar{v}_i$ is finite. This completes the proof. $\qquad\square$

In order to investigate the consistency, we are now here to provide the discretization error of the collisional nonlinear breakage equation by cell average volume method as follows.

3.4. Discretization error.

The spatial truncation error is given by for $i = 1, 2, \ldots, I$,

(3.23)
$$
\sigma_i(t) = \frac{\mathrm{d}N_i(t)}{\mathrm{d}t} - \frac{\mathrm{d}\hat{N}_i(t)}{\mathrm{d}t} = \left[B_i(t) - \hat{\mathcal{B}}_i(t)\right] - \left[D_i(t) - \hat{\mathcal{D}}_i(t)\right]
$$

We can write
(3.24)
$$
\sigma_i(t) = \begin{cases}
C_i\left(\dfrac{\Delta x_i^2}{\Delta x_i + \Delta x_{i+1}} - \dfrac{\Delta x_{i-1}^2}{\Delta x_i + \Delta x_{i-1}}\right) + \mathcal{O}(\Delta x_i^2), & \text{if} \quad \bar{v}_{i-1} > x_{i-1}, \ \ \bar{v}_i > x_i, \ \ \bar{v}_{i+1} \geq x_{i+1}, \\[2ex]
C_i\left(\dfrac{\Delta x_{i+1}^2}{\Delta x_i + \Delta x_{i+1}} - \dfrac{\Delta x_i^2}{\Delta x_i + \Delta x_{i-1}}\right) + \mathcal{O}(\Delta x_i^2), & \text{if} \quad \bar{v}_{i-1} \leq x_{i-1}, \ \ \bar{v}_i < x_i, \ \ \bar{v}_{i+1} < x_{i+1}, \\[2ex]
\mathcal{O}(\Delta x_i^3), & \text{if} \quad \bar{v}_{i-1} \leq x_{i-1}, \ \ \bar{v}_i = x_i, \ \ \bar{v}_{i+1} \geq x_{i+1}, \\[2ex]
\mathcal{O}(\Delta x_i^2), & \text{else,} \quad i = 1, I_1, I_2, \ldots, I_m, I,
\end{cases}
$$

where

$$
C_i = \frac{1}{4}\sum_{k=1}^{I} F(x_i|x_i;x_k)\hat{N}_i(t)\hat{N}_k(t).
$$

Remark 3.2. Extending the Remark 3.1, the spatial truncation error is obtained as

(3.25)
$$\sigma_i(t) = \begin{cases} C_i'\left(\dfrac{\Delta x_i^3}{\Delta x_i + \Delta x_{i+1}} - \dfrac{\Delta x_{i-1}^3}{\Delta x_i + \Delta x_{i-1}}\right) + \mathcal{O}(\Delta x_i^3), & \text{if} \quad \bar{v}_{i-1} > x_{i-1}, \ \ \bar{v}_i > x_i, \ \ \bar{v}_{i+1} \geq x_{i+1}, \\[2em] C_i'\left(\dfrac{\Delta x_{i+1}^3}{\Delta x_i + \Delta x_{i+1}} - \dfrac{\Delta x_i^3}{\Delta x_i + \Delta x_{i-1}}\right) + \mathcal{O}(\Delta x_i^3), & \text{if} \quad \bar{v}_{i-1} \leq x_{i-1}, \ \ \bar{v}_i < x_i, \ \ \bar{v}_{i+1} < x_{i+1}, \\[2em] \mathcal{O}(\Delta x_i^3), & \text{if} \quad \bar{v}_{i-1} \leq x_{i-1}, \ \ \bar{v}_i = x_i, \ \ \bar{v}_{i+1} \geq x_{i+1}, \\[2em] \mathcal{O}(\Delta x_i^3), & \text{else}, \quad i = 1, I_1, I_2, \ldots, I_m, I, \end{cases}$$

where

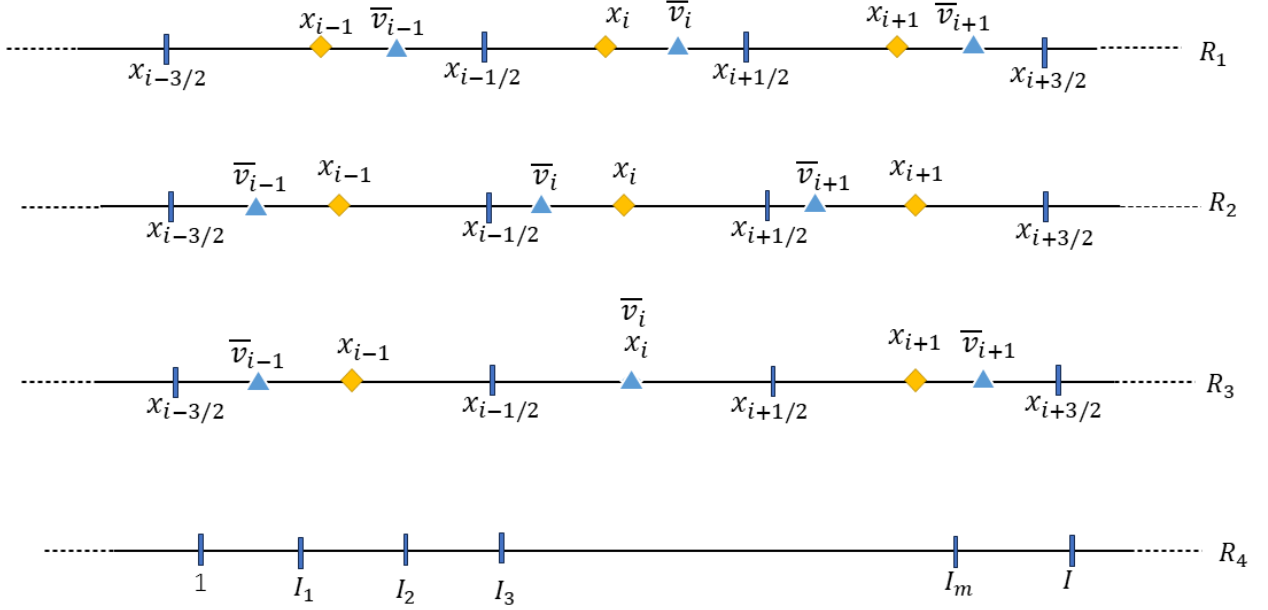$$C_i' = -\frac{1}{6}\sum_{k=1}^{I}\sum_{j=i+2}^{I} F_x(x_i|x_j; x_k)\hat{N}_j(t)\hat{N}_k(t).$$

FIGURE 4. Four different set of regions

Here, the four cases arise for the order of local error. The last case arises due to the sign change of $x_i - \bar{v}_i$ and due to outer boundaries. Lemma 3.3 provides that the number of the sign changes of $x_i - \bar{v}_i$ depends on the properties of the birth rate function $B(x, t)$. Since the sign of $x_i - \bar{v}_i$ changes in m cells, say, $I_1, I_2, \ldots, I_m$, so the order may deteriorate. Here, the number of cells remains finite, so the it does not lower the order of the numerical scheme. In simplified form, we describe four cases as follows: (see Figure 4)

$$\begin{aligned} R_1 &:= \{i \in \mathbb{N} : \bar{v}_{i-1} > x_{i-1}, \ \ \bar{v}_i > x_i, \ \ \bar{v}_{i+1} \geq x_{i+1}\}, \\ R_2 &:= \{i \in \mathbb{N} : \bar{v}_{i-1} \leq x_{i-1}, \ \ \bar{v}_i < x_i, \ \ \bar{v}_{i+1} < x_{i+1}\}, \\ R_3 &:= \{i \in \mathbb{N} : \bar{v}_{i-1} \leq x_{i-1}, \ \ \bar{v}_i = x_i, \ \ \bar{v}_{i+1} \geq x_{i+1}\}, \\ R_4 &:= \{i \in \mathbb{N} : i = 1, I_1, I_2, \ldots, I_m, I\}. \end{aligned}$$

Then, the order of consistency is

$$\|\sigma(t)\| = \sum_{i \in R_1} |\sigma_i(t)| \sum_{i \in R_2} |\sigma_i(t)| + \sum_{i \in R_3} |\sigma_i(t)| + \sum_{i \in R_4} |\sigma_i(t)|$$

$$= \sum_{i \in R_1} \left| C_i \left(\frac{\Delta x_i^2}{\Delta x_i + \Delta x_{i+1}} - \frac{\Delta x_{i-1}^2}{\Delta x_i + \Delta x_{i-1}} \right) \right| + \sum_{i \in R_2} \left| C_i \left(\frac{\Delta x_{i+1}^2}{\Delta x_i + \Delta x_{i+1}} - \frac{\Delta x_i^2}{\Delta x_i + \Delta x_{i-1}} \right) \right|$$

$$+ |\sigma_1(t)| + (|\sigma_{I_1}(t)| + |\sigma_{I_2}(t)| + \cdots + |\sigma_{I_m}(t)|) + |\sigma_I(t)| + \mathcal{O}(\Delta x^2)$$

$$= \sum_{i \in R_1} \left| C_i \left(\frac{\Delta x_i^2}{\Delta x_i + \Delta x_{i+1}} - \frac{\Delta x_{i-1}^2}{\Delta x_i + \Delta x_{i-1}} \right) \right| + \sum_{i \in R_2} \left| C_i \left(\frac{\Delta x_{i+1}^2}{\Delta x_i + \Delta x_{i+1}} - \frac{\Delta x_i^2}{\Delta x_i + \Delta x_{i-1}} \right) \right|$$
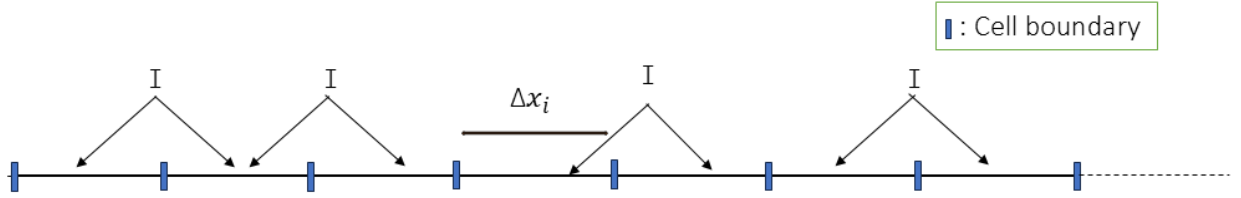
$$\text{(3.26)} \qquad + \mathcal{O}(\Delta x).$$

FIGURE 5. Uniform smooth grids

3.4.1. *Type A: Uniform grids.* Over uniform grids, shown in Figure 5, $\Delta x_i = \Delta x$ for $i = 1, 2, \ldots, I$. From (3.26) we obtain

$$\text{(3.27)} \qquad \|\sigma(t)\| = \mathcal{O}(\Delta x).$$

3.4.2. *Type B: Nonuniform smooth grids.* Consider a smooth transformation $x = f(\varphi)$ to get nonuniform grid (see in Figure 6),
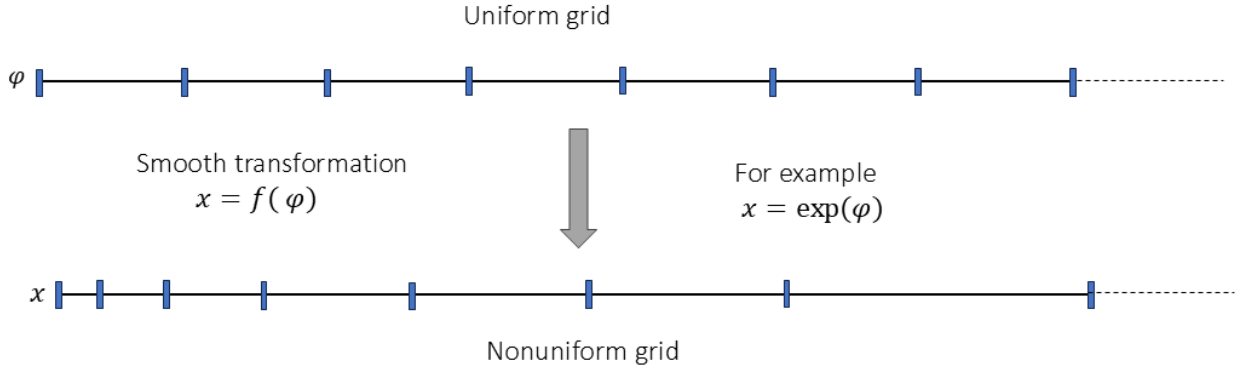

FIGURE 6. Nonuniform smooth grids

where $x_{i \pm 1/2} = f(\varphi_i \pm h/2)$ for all $i = 1, 2, \ldots, I$ and ϕ is a variable with uniform grids and let h be the uniform grid width in the variable ϕ. Now expanding the Taylor's series of f, we get

$$\Delta x_i = x_{i+1/2} - x_{i-1/2} = f(\varphi_i + h/2) - f(\varphi_i - h/2) = h f'(\varphi_i) + \frac{h^3}{24} f'''(\varphi_i) + \mathcal{O}(h^4).$$

Analogously, we obtain

$$\Delta x_{i+1} = x_{i+3/2} - x_{i+1/2} = f(\varphi_i + 3h/2) - f(\varphi_i + h/2) = h f'(\varphi_i) + h^2 f''(\varphi_i) + \mathcal{O}(h^3)$$

and

$$\Delta x_{i-1} = x_{i-1/2} - x_{i-3/2} = f(\varphi_i - h/2) - f(\varphi_i - 3h/2) = h f'(\varphi_i) - h^2 f''(\varphi_i) + \mathcal{O}(h^3).$$

By above approximations we have

$$\Delta x_i + \Delta x_{i-1} = 2h f'(\varphi_i) - h^2 f''(\varphi_i) + \mathcal{O}(h^3),$$
$$\Delta x_i + \Delta x_{i+1} = 2h f'(\varphi_i) + h^2 f''(\varphi_i) + \mathcal{O}(h^3).$$

We can get from the first term as

$$\frac{\Delta x_i^2}{\Delta x_i + \Delta x_{i+1}} - \frac{\Delta x_{i-1}^2}{\Delta x_i + \Delta x_{i-1}} = \frac{2h^3 (f'(\varphi_i))^3 - 2h^3 (f'(\varphi_i))^3 + \mathcal{O}(h^4)}{\mathcal{O}(h^2)} = \mathcal{O}(h^2).$$

Similarly,

$$\frac{\Delta x_{i+1}^2}{\Delta x_i + \Delta x_{i+1}} - \frac{\Delta x_i^2}{\Delta x_i + \Delta x_{i-1}} = \mathcal{O}(h^2).$$

Therefore,

$$\frac{\Delta x_i^2}{\Delta x_i + \Delta x_{i+1}} - \frac{\Delta x_{i-1}^2}{\Delta x_i + \Delta x_{i-1}} = \mathcal{O}(\Delta x_i^2) \text{ and } \frac{\Delta x_{i+1}^2}{\Delta x_i + \Delta x_{i+1}} - \frac{\Delta x_i^2}{\Delta x_i + \Delta x_{i-1}} = \mathcal{O}(\Delta x_i^2).$$

From (3.26) and the above estimates, we obtain
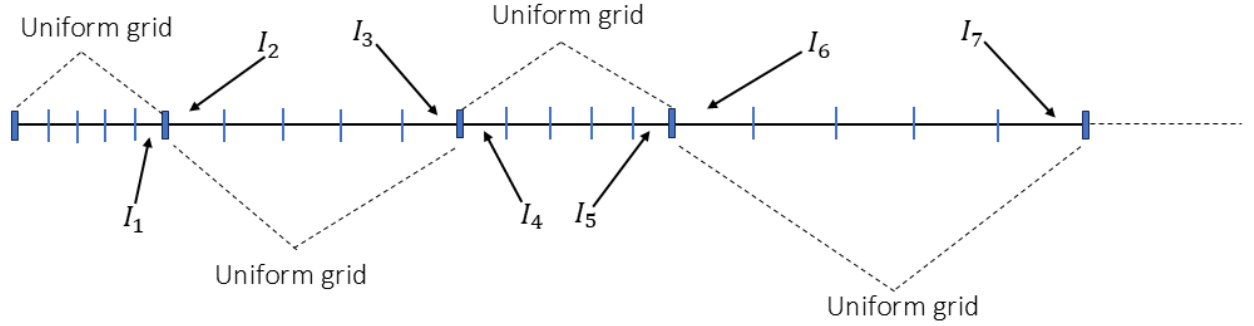
$$||\sigma(t)|| = \mathcal{O}(\Delta x).$$

FIGURE 7. Locally-uniform smooth grids

3.4.3. *Type C: Locally-uniform grids.* Over locally-uniform grids, shown in Figure 7, from (3.26) we obtain

$$(3.28) \qquad \sigma_i(t) = \begin{cases} \mathcal{O}(\Delta x_i^2), & \text{for } i = 1, I_1, I_2, \ldots, I_m, I, \\ \mathcal{O}(\Delta x_i^3) & \text{elsewhere.} \end{cases}$$

Therefore, the order of consistency is given by

$$(3.29) \qquad\qquad ||\sigma(t)|| = \mathcal{O}(\Delta x).$$

3.4.4. *Type D: Random grids.* Over random grids, no leading expressions are going to vanish in (3.26). From **Case I**, we consider first leading term by using the relation $\dfrac{\Delta x}{\Delta x_{\min}} \leq \alpha$

$$\frac{\Delta x_i^2}{\Delta x_i + \Delta x_{i+1}} C_i + \mathcal{O}(\Delta x_i^2) \leq \frac{\Delta x^2}{\Delta x_{\min}} + \mathcal{O}(\Delta x_i^2) \leq \alpha \Delta x + \mathcal{O}(\Delta x_i^2).$$

Similar argument is applicable for **Case II**. Therefore, from (3.26) we can easily say that the order of consistency is

$$(3.30) \qquad\qquad ||\sigma(t)|| = \mathcal{O}(\Delta x).$$

3.4.5. *Type E: Oscillatory grids.* In order to track the oscillatory behavior (unlikely event) in discretized points due to the effect of collisions, let us consider oscillatory grids defined as

$$\Delta x_{i+1} := \begin{cases} \frac{1}{2}\Delta x_i, & \text{if } i \text{ is even} \\ 2\Delta x_i & \text{if } i \text{ is odd.} \end{cases}$$

By performing this above defined oscillatory grids in (3.26), we obtain

$$||\sigma(t)|| = \mathcal{O}(\Delta x).$$

Therefore, we can say that VAM is first order consistent on oscillatory grids.

Remark 3.3. It is observed that over uniform, nonuniform and locally-uniform grids, the VAM executes first order consistency same as the FPT [11]. Over random grids, VAM exhibits first-order consistency, whereas the FPT becomes inconsistent over random grids [11]. This employs that VAM offers better accuracy in terms of consistency compared to FPT for solving the collisional nonlinear breakage equation over random grids. Furthermore, it is found that VAM achieves first-order consistency by applying to oscillatory grids.

Remark 3.4. Compiling the Remark 3.1 and 3.2, we compute the spacial truncation error over all four different regions R_1, R_2, R_3, R_4. The order of consistency is obtained as

$$\begin{aligned}
||\sigma(t)|| &= \sum_{i \in R_1} |\sigma_i(t)| \sum_{i \in R_2} |\sigma_i(t)| + \sum_{i \in R_3} |\sigma_i(t)| + \sum_{i \in R_4} |\sigma_i(t)| \\
&= \sum_{i \in R_1} \left| C_i' \left(\frac{\Delta x_i^3}{\Delta x_i + \Delta x_{i+1}} - \frac{\Delta x_{i-1}^3}{\Delta x_i + \Delta x_{i-1}} \right) \right| + \sum_{i \in R_2} \left| C_i' \left(\frac{\Delta x_{i+1}^3}{\Delta x_i + \Delta x_{i+1}} - \frac{\Delta x_i^3}{\Delta x_i + \Delta x_{i-1}} \right) \right| \\
&\quad + |\sigma_1(t)| + (|\sigma_{I_1}(t)| + |\sigma_{I_2}(t)| + \cdots + |\sigma_{I_m}(t)|) + |\sigma_I(t)| + \mathcal{O}(\Delta x^2) \\
&= \sum_{i \in R_1} \left| C_i' \left(\frac{\Delta x_i^3}{\Delta x_i + \Delta x_{i+1}} - \frac{\Delta x_{i-1}^3}{\Delta x_i + \Delta x_{i-1}} \right) \right| + \sum_{i \in R_2} \left| C_i' \left(\frac{\Delta x_{i+1}^3}{\Delta x_i + \Delta x_{i+1}} - \frac{\Delta x_i^3}{\Delta x_i + \Delta x_{i-1}} \right) \right| \\
&\quad + \mathcal{O}(\Delta x^2).
\end{aligned}$$

(3.31)

Thus VAM shows second order consistency that is $||\sigma(t)|| = \mathcal{O}(\Delta x^2)$ over uniform, nonuniform and locally-uniform grids, whereas $||\sigma(t)|| = \mathcal{O}(\Delta x)$ over random and oscillatory grids.

3.5. **Convergence.** To prove the consistency and convergence of the new scheme VAM, the following theorem is utilized.

Theorem 3.2. *[Convergence theorem] Assume that the mapping $\hat{J}$ satisfies Lipschitz condition for $0 \leq t \leq T$ and for all $N, \hat{N} \in \mathbb{R}^I$ where N and $\hat{N}$ are projected exact and numerical solutions defined in (2.4) and (2.14) respectively. Then a consistent discretization method is also convergent and the order of the convergence is the same order as the consistency.*

Proof. Let $\boldsymbol{E}(t)$ be the global discretization error and is defined by $\boldsymbol{E}(t) = \boldsymbol{N}(t) - \hat{\boldsymbol{N}}(t)$ for all $\boldsymbol{N}, \hat{\boldsymbol{N}} \in \mathbb{R}^I$. Now, we can write

$$(3.32) \qquad \frac{\mathrm{d}\boldsymbol{E}(t)}{\mathrm{d}t} = \frac{\mathrm{d}\boldsymbol{N}(t)}{\mathrm{d}t} - \frac{\mathrm{d}\hat{\boldsymbol{N}}(t)}{\mathrm{d}t} = \hat{\boldsymbol{J}}(\boldsymbol{N}(t)) - \hat{\boldsymbol{J}}(\hat{\boldsymbol{N}}(t)).$$

From Proposition 3.1, $\hat{\boldsymbol{J}}$ satisfies Lipschitz condition, so there exist Lipschitz constant $\gamma < \infty$ such that

$$(3.33) \qquad ||\hat{\boldsymbol{J}}(\boldsymbol{N}) - \hat{\boldsymbol{J}}(\hat{\boldsymbol{N}})|| \leq \gamma ||\boldsymbol{N} - \hat{\boldsymbol{N}}|| \quad \text{for all } \boldsymbol{N}, \hat{\boldsymbol{N}} \in \mathbb{R}^I.$$

Using Lipschitz condition (3.33) in (3.32), we obtain

$$(3.34) \qquad \frac{\mathrm{d}||\boldsymbol{E}(t)||}{\mathrm{d}t} \leq ||\hat{\boldsymbol{J}}(\boldsymbol{N}(t)) - \hat{\boldsymbol{J}}(\hat{\boldsymbol{N}}(t))|| \leq \gamma ||\boldsymbol{N} - \hat{\boldsymbol{N}}|| = \gamma ||\boldsymbol{E}(t)||.$$

The above inequality implies that

$$(3.35) \qquad ||\boldsymbol{E}(t)|| \leq ||\boldsymbol{E}(0)|| \exp(\gamma t).$$

When $\Delta x \to 0$, with the relation $||\boldsymbol{E}(0)|| = 0$ and by the definition of global dicretization error, we deduce that $||\boldsymbol{E}(t)|| = 0$ that is if the new discretization method is consistent, then it is convergent and the order of the convergence is same as the order of consistency. □

Thus, from the convergence theorem 3.2, we can say that the numerical VAM (2.14) is convergent and the order of convergence of the VAM is same as the order of consistency.

4. Two-dimensional collisional breakage equation

In particulate process, a particle is characterized by different properties such as volume, energy, moisture content etc. These properties need to be defined by more than one-dimension. Here, we assume two particle properties x_1 and x_2. The corresponding collisional nonlinear breakage equation in two particle properties (or dimensions)is written as

$$\frac{\partial n(x_1, x_2, t)}{\partial t} = \int_0^\infty \int_0^\infty \int_{x_1}^\infty \int_{x_2}^\infty \beta(x_1, x_2 | y_1, y_2; z_1, z_2) \mathcal{K}(y_1, y_2, z_1, z_2) n(y_1, y_2, t) n(z_1, z_2, t) \mathrm{d}y_2 \mathrm{d}y_1 \mathrm{d}z_2 \mathrm{d}z_1$$

$$(4.1) \qquad - n(x_1, x_2, t) \int_0^\infty \int_0^\infty \mathcal{K}(x_1, x_2, y_1, y_2) n(y_1, y_2, t) \mathrm{d}y_2 \mathrm{d}y_1,$$

with the initial condition

$$(4.2) \qquad n(x_1, x_2, 0) = n_0(x_1, x_2) \geq 0, \quad \text{for} \quad (x_1, x_2) \in \mathbb{R}^+ \times \mathbb{R}^+.$$

Here, all the functions present in equation (4.1) are defined similar to the one-dimensional collisional nonlinear breakage equation. The moments of the particles with properties x_1 and x_2 is given by

$$(4.3) \qquad \mathcal{M}_{r_1, r_2}(t) = \int_0^\infty \int_0^\infty x_1^{r_1} x_2^{r_2} n(x_1, x_2, t) \mathrm{d}x_2 \mathrm{d}x_1, \quad \text{for all} \quad r_1, r_2 = 0, 1, 2, \dots.$$

Here, the zeroth order moment $\mathcal{M}_{0,0}(t)$ represents the total number of particles, whereas the moments $\mathcal{M}_{1,0}(t)$ and $\mathcal{M}_{0,1}(t)$ denotes the total amount of property with respect to x_1 and x_2, respectively and the moment $\mathcal{M}_{1,1}(t)$ describes the hypervolume of the particles.

We truncate the model in the finite computational domain $[0, x_{\max}]^2$ with $x_{\max} < \infty$ and the time is taken as $[0, T]$. Next we discretize the computational domain as cartesian grid into $I_1 I_2$ cells as $\Lambda_{i,j} := [x_{1,i-1/2}, x_{1,i+1/2}] \times [x_{2,j-1/2}, x_{2,j+1/2}]$ with $1 \leq i \leq I_1$ and $1 \leq j \leq I_2$. Moreover,

$$x_{1,1/2} := 0, \quad x_{2,1/2} := 0, \quad x_{1,I_1+1/2} := R_1 \quad \text{and} \quad x_{2,I_2+1/2} := R_2.$$

The representative of the particle population in the cell (i, j) is denoted by $(x_{1,i}, x_{2,j})$ where

$$x_{1,i} := \frac{x_{1,i-1/2} + x_{1,i+1/2}}{2} \quad \text{and} \quad x_{2,j} := \frac{x_{2,j-1/2} + x_{2,j+1/2}}{2},$$

and also

$$\Delta x_{1,i} := x_{1,i+1/2} - x_{1,i-1/2} \quad \text{and} \quad \Delta x_{2,j} := x_{2,j+1/2} - x_{2,j-1/2}.$$

Let $N_{i,j}(t)$ be the discrete number density in $\Lambda_{i,j}$ at time t is defined by

$$(4.4) \qquad N_{i,j}(t) = \int_{\Lambda_{i,j}} n(x_1, x_2, t) \mathrm{d}x_2 \mathrm{d}x_1.$$

Integrating equation truncated equation (4.1) with respect to the volume variables $x_{1,i}$ and $x_{2,j}$ over each cell $\Lambda_{i,j}$, we obtain

$$(4.5) \qquad \frac{\mathrm{d}N_{i,j}(t)}{\mathrm{d}t} = B_{i,j}(t) - D_{i,j}(t).$$

Here, $B_{i,j}(t)$ is the birth rate and $D_{i,j}(t)$ is the death rate of particles and are given by

$$B_{i,j}(t) := \int_{\Lambda_{i,j}} \int_0^{R_1} \int_0^{R_2} \int_{x_1}^{R_1} \int_{x_2}^{R_2} \beta(x_1, x_2 | y_1, y_2; z_1, z_2) \mathcal{K}(y_1, y_2, z_1, z_2)$$

$$(4.6a) \qquad\qquad\qquad \times n(y_1, y_2, t) n(z_1, z_2, t) \mathrm{d}y_2 \mathrm{d}y_1 \mathrm{d}z_2 \mathrm{d}z_1 \mathrm{d}x_2 \mathrm{d}x_1,$$

and

$$(4.6b) \qquad D_{i,j}(t) := \int_{\Lambda_{i,j}} \int_0^{R_1} \int_0^{R_2} \mathcal{K}(x_1, x_2, y_1, y_2) n(x_1, x_2, t) n(y_1, y_2, t) \mathrm{d}y_2 \mathrm{d}y_1 \mathrm{d}x_2 \mathrm{d}x_1.$$

Putting $n(x_1, x_2, t) \approx \sum_{i=1}^{I_1} \sum_{i=1}^{I_2} N_{i,j}(t) \delta(x - x_{1,i}) \delta(x - x_{2,j})$ in the above equations (4.5)-(4.6), we get the discrete formulation of two-dimensional collisional nonlinear breakage equation as

$$(4.7) \qquad \frac{\mathrm{d}N_{i,j}(t)}{\mathrm{d}t} = \hat{B}_{i,j}(t) - \hat{D}_{i,j}(t),$$

where $\hat{N}_i(t)$ discrete approximation of the density function at time $t \geq 0$. Here, birth terms and death terms are defined by

$$(4.8\mathrm{a}) \qquad \hat{B}_{i,j}(t) := \sum_{p_1=1}^{I_1} \sum_{p_2=1}^{I_2} \sum_{q_1=i}^{I_1} \sum_{q_2=j}^{I_2} \beta_{i,j}^{q_1,q_2} \mathcal{K}(x_{1,q_1}, x_{2,q_2}, x_{1,p_1}, x_{2,p_2}) N_{q_1,q_2}(t) N_{p_1,p_2}(t),$$

$$(4.8\mathrm{b}) \qquad \hat{D}_{i,j}(t) := \sum_{p_1=1}^{I_1} \sum_{p_2=1}^{I_2} \mathcal{K}(x_{1,i}, x_{2,j}, x_{1,p_1}, x_{2,p_2}) N_{i,j}(t) N_{p_1,p_2}(t),$$

where $\beta_{i,j}^{q_1,q_2} = \int_{x_{1,i-1/2}}^{p_{1,i}^{q_1}} \int_{x_{2,j-1/2}}^{p_{2,j}^{q_2}} \beta(x_1, x_2 | x_{1,q_1}, x_{2,q_2}; x_{1,p_1}, x_{2,p_2}) \mathrm{d}x_2 \mathrm{d}x_1$ and for all $k = 1, 2$ with $l = i, j$,

$$p_{k,l}^{q_k} = \begin{cases} x_{k,l}, & \text{if} \quad q_k = l, \\ x_{k,l+1/2}, & \text{otherwise.} \end{cases}$$

The total mass flux of the property for x_1 and x_2, respectively over $\Lambda_{i,j}$ are given by

$$
\begin{aligned}
V_{x_1,i}(t) := \int_{\Lambda_{i,j}} \int_0^{R_1} \int_0^{R_2} \int_{x_1}^{R_1} \int_{x_2}^{R_2} & x_1 \beta(x_1, x_2 | y_1, y_2; z_1, z_2) \mathcal{K}(y_1, y_2, z_1, z_2) \\
(4.9) & \times n(y_1, y_2, t) n(z_1, z_2, t) \mathrm{d}y_2 \mathrm{d}y_1 \mathrm{d}z_2 \mathrm{d}z_1 \mathrm{d}x_2 \mathrm{d}x_1,
\end{aligned}
$$

and

$$
\begin{aligned}
V_{x_2,i}(t) := \int_{\Lambda_{i,j}} \int_0^{R_1} \int_0^{R_2} \int_{x_1}^{R_1} \int_{x_2}^{R_2} & x_2 \beta(x_1, x_2 | y_1, y_2; z_1, z_2) \mathcal{K}(y_1, y_2, z_1, z_2) \\
(4.10) & \times n(y_1, y_2, t) n(z_1, z_2, t) \mathrm{d}y_2 \mathrm{d}y_1 \mathrm{d}z_2 \mathrm{d}z_1 \mathrm{d}x_2 \mathrm{d}x_1.
\end{aligned}
$$

The discrete mass flux of property for x_1 and x_2, respectively over $\Lambda_{i,j}$ are obtained as

$$
\begin{aligned}
\hat{V}_{x_1,i}(t) := \sum_{p_1=1}^{I_1} \sum_{p_2=1}^{I_2} \sum_{q_1=i}^{I_1} \sum_{q_2=j}^{I_2} & \mathcal{K}(x_{1,q_1}, x_{2,q_2}, x_{1,p_1}, x_{2,p_2}) N_{q_1,q_2}(t) N_{p_1,p_2}(t) \\
(4.11) & \times \int_{x_{1,i-1/2}}^{p_{1,i}^{q_1}} \int_{x_{2,j-1/2}}^{p_{2,j}^{q_2}} x_1 \beta(x_1, x_2 | x_{1,q_1}, x_{2,q_2}; x_{1,p_1}, x_{2,p_2}) \mathrm{d}x_2 \mathrm{d}x_1,
\end{aligned}
$$

and

$$
\begin{aligned}
\hat{V}_{x_2,j}(t) := \sum_{p_1=1}^{I_1} \sum_{p_2=1}^{I_2} \sum_{q_1=i}^{I_1} \sum_{q_2=j}^{I_2} & \mathcal{K}(x_{1,q_1}, x_{2,q_2}, x_{1,p_1}, x_{2,p_2}) N_{q_1,q_2}(t) N_{p_1,p_2}(t) \\
(4.12) & \times \int_{x_{1,i-1/2}}^{p_{1,i}^{q_1}} \int_{x_{2,j-1/2}}^{p_{2,j}^{q_2}} x_2 \beta(x_1, x_2 | x_{1,q_1}, x_{2,q_2}; x_{1,p_1}, x_{2,p_2}) \mathrm{d}x_2 \mathrm{d}x_1.
\end{aligned}
$$

The average property values of all new born particles for property with respect to x_1 and x_2, respectively in $\Lambda_{i,j}$ are given by

$$(4.13) \qquad \bar{v}_{1,i} := \frac{\hat{V}_{x_1,i}}{\hat{B}_{i,j}} \quad \text{and} \quad \bar{v}_{2,j} := \frac{\hat{V}_{x_2,j}}{\hat{B}_{i,j}}.$$

Similar argument is used as one-dimensional case to formulate the numerical scheme VAM.

Here, $\hat{\boldsymbol{N}} = \left\{ \hat{N}_{i,j} \right\} \in \mathbb{R}^{I_1} \times \mathbb{R}^{I_2}$ be nonnegative vector for $i = 1, 2, \ldots, I_1$ and $j = 1, 2, \ldots, I_2$.

4.1. **Cell volume average method in two-dimension.** The numerical scheme for two-dimensional collisional nonlinear breakage equation by VAM is defined by

$$\frac{\mathrm{d}\hat{N}_{i,j}(t)}{\mathrm{d}t} = \sum_{p=0}^{1}\sum_{q=0}^{1} \lambda_{i,j}^{-;-}(\bar{v}_{1,i-p}, \bar{v}_{2,j-q}) H[(-1)^p(x_{1,i-p} - \bar{v}_{1,i-p})] H[(-1)^q(x_{2,j-q} - \bar{v}_{2,j-q})]\hat{B}_{i-p,j-q}(t)$$

$$+ \sum_{p=0}^{1}\sum_{q=0}^{1} \lambda_{i,j}^{-;+}(\bar{v}_{1,i-p}, \bar{v}_{2,j+q}) H[(-1)^p(x_{1,i-p} - \bar{v}_{1,i-p})] H[(-1)^q(x_{2,j+q} - \bar{v}_{2,j+q})]\hat{B}_{i-p,j+q}(t)$$

$$+ \sum_{p=0}^{1}\sum_{q=0}^{1} \lambda_{i,j}^{+;-}(\bar{v}_{1,i+p}, \bar{v}_{2,j-q}) H[(-1)^p(x_{1,i+p} - \bar{v}_{1,i+p})] H[(-1)^q(x_{2,j-q} - \bar{v}_{2,j-q})]\hat{B}_{i+p,j-q}(t)$$

$$+ \sum_{p=0}^{1}\sum_{q=0}^{1} \lambda_{i,j}^{+;+}(\bar{v}_{1,i+p}, \bar{v}_{2,j+q}) H[(-1)^p(x_{1,i+p} - \bar{v}_{1,i+p})] H[(-1)^q(x_{2,j+q} - \bar{v}_{2,j+q})]\hat{B}_{i+p,j+q}(t)$$

$$(4.14) \qquad - \sum_{p=1}^{I_{x_1}}\sum_{q=1}^{I_{x_2}} \mathcal{K}(x_{1,i}, x_{1,p}, x_{2,j}, x_{2,q})\hat{N}_{i,j}\hat{N}_{p,q},$$

where $\hat{B}_{i,j}(t)$ defined by (4.8) and $\lambda_{i,j}^{\pm;\pm}(\bar{v}_{1,i}, \bar{v}_{2,j}) := \dfrac{(\bar{v}_{1,i} - x_{1,i\pm1})(\bar{v}_{2,j} - x_{2,j\pm1})}{(x_{1,i} - x_{1,i\pm1})(x_{2,j} - x_{2,j\pm1})}$ and H is the Heaviside function defined as in previous one-dimensional case.

5. Numerical discussion

This section is devoted to examine the accuracy of VAM against existing fixed pivot technique and exact results for particular initial conditions to solve the collisional nonlinear breakage equation. This section is divided in two sub parts based on dimensions of the collisional nonlinear breakage equation. For one dimensional problem, two and for multi-dimensional PBEs, two test cases are analyzed. To access the accuracy and versatility of VAM, the results are compared with the exact values and FPT based approximations. For the numerical validation both thematic and data analysis is carried out.

5.1. **One-dimensional case.** This part deals with the one-dimensional numerical results with two test examples together with a detailed error estimations between the new scheme VAM and FPT. Additionally, we show comparison with exact solutions. The significant key finding is that the VAM performs much better than existing fixed pivot techniques [11] over random grids. The relative errors of the moments are calculated using the following relation

$$(5.1) \qquad E_{\mathcal{M}_r}(t) = \left| \frac{\mathcal{M}_r(t) - \hat{\mathcal{M}}_r(t)}{\mathcal{M}_r(t)} \right|.$$

Here, $\mathcal{M}_r(t)$ and $\hat{\mathcal{M}}_r(t)$ are the exact and numerical value of the rth moment, respectively.

During numerical computations, dimensionless values are considered of all the concerned quantities which are obtained by dividing the quantities with corresponding initial values. The computational domain for particle size is taken as $D := [10^{-9}, 1]$ and it is discretized into 30 nonuniform sub-intervals using the geometric recurrence relation $x_{i+1/2} = rx_{i-1/2}$, where $r = 1.4$. All simulations are performed in a HP Z6 G4 workstation and using MATLAB R2023b software.

Test case 5.1. *Consider collisional nonlinear breakage equation with monodispresed initial condition* $n(x,0) = \begin{cases} 1, & x=1 \\ 0, & otherwise \end{cases}$ *with collisional kernel* $\mathcal{K}(x,y) = xy$ *and breakage function as* $\beta(x|y;z) = \dfrac{2}{y}$. *This breakage function splits the mother particle into two daughter particles.*

Figure 8 is the particle number density function representation at time $t = 1$ in log scale for three different type of grids. For nonuniform grid, FPT and VAM both predict number density with high accuracy and are inline the exact one as shown in Figure 8a. However, when Locally-uniform grids are considered, FPT over-predicted number density at few points and VAM generated accurate results (refer to Figure 8b). Moreover, from Figure 8c for random grid type FPT seems to fail in approximating the density function. On the other

hand, VAM produced satisfactory results. To summarize, we can say that irrespective of grid type, VAM gives highly efficient solution.

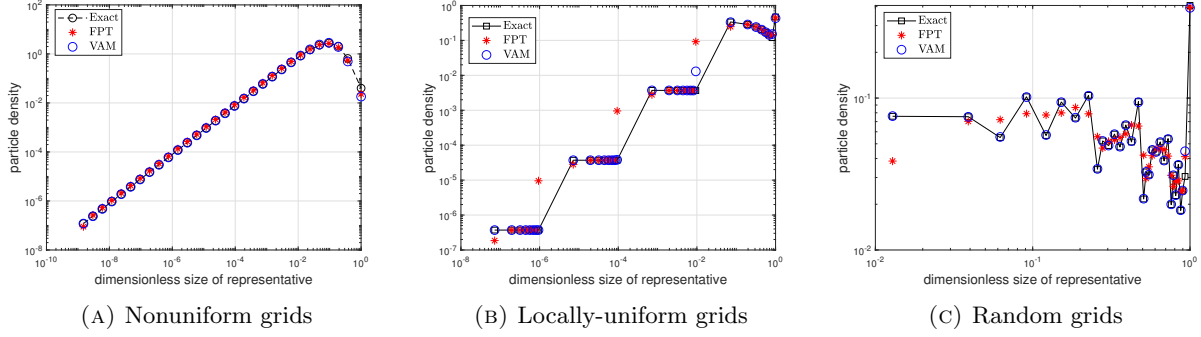(A) Nonuniform grids   (B) Locally-uniform grids   (C) Random grids

FIGURE 8. Comparison of number density for different grid types at $t = 1$ for test case 5.1.

Different order moments are calculated over nonuniform grids. Since, over locally-uniform and random grids, FPT fails to predict number density, therefore they are not considered for moments calculation. The zeroth and first order moments are depicted in Figure 9a and both are inline with the exact and FPT based moments. Table 1 supports the insignificant error claim. Second and third moment is plotted in Figure 9b and 9c. Moment error data is presented in Table 1. As compared to FPT, the new scheme VAM produces more accurate results.
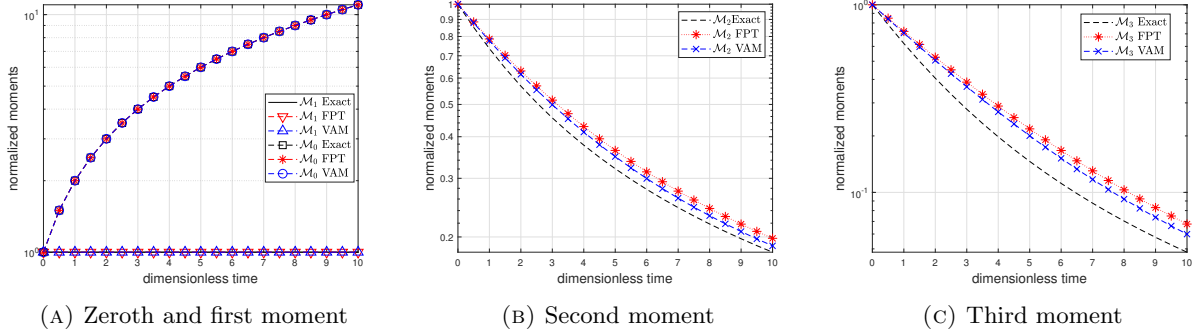

(A) Zeroth and first moment   (B) Second moment   (C) Third moment

FIGURE 9. Different order moments for test case 5.1.

Method	VAM			FPT		
Time	$E_{\mathcal{M}_0}$	$E_{\mathcal{M}_1}$	$E_{\mathcal{M}_2}$	$E_{\mathcal{M}_0}$	$E_{\mathcal{M}_1}$	$E_{\mathcal{M}_2}$
2	1.43×10^{-9}	8.23×10^{-9}	8.46×10^{-2}	2.76×10^{-9}	8.23×10^{-9}	1.12×10^{-1}
4	5.56×10^{-9}	8.29×10^{-8}	1.37×10^{-1}	3.17×10^{-9}	8.29×10^{-8}	9.46×10^{-2}
6	5.91×10^{-9}	4.26×10^{-8}	1.28×10^{-1}	2.49×10^{-9}	4.26×10^{-8}	7.78×10^{-2}
8	3.02×10^{-9}	7.62×10^{-8}	5.88×10^{-2}	7.44×10^{-9}	7.62×10^{-8}	1.13×10^{-1}
10	3.53×10^{-9}	9.29×10^{-8}	4.49×10^{-2}	8.96×10^{-9}	9.29×10^{-8}	1.01×10^{-1}

TABLE 1. Error analysis of different order moments for test case 5.1.

Test case 5.2. *Consider collisional nonlinear breakage equation with monodispresed initial condition with collisional kernel $\mathcal{K}(x, y) = 1$ and breakage function as $\beta(x|y; z) = \dfrac{4x^2}{y^3}$.*

Particle number density in log scale at time $t = 1$ is presented in the Figure 10 for three type of grids. For small particle sizes, FPT under-predicts it whereas VAM gives accurate approximation for nonuniform grids. For locally-uniform and random grids, FPT fails predicts the density function as shown in Figure 10b and 10c, respectively. However, VAM produces more accurate results for both grid types.

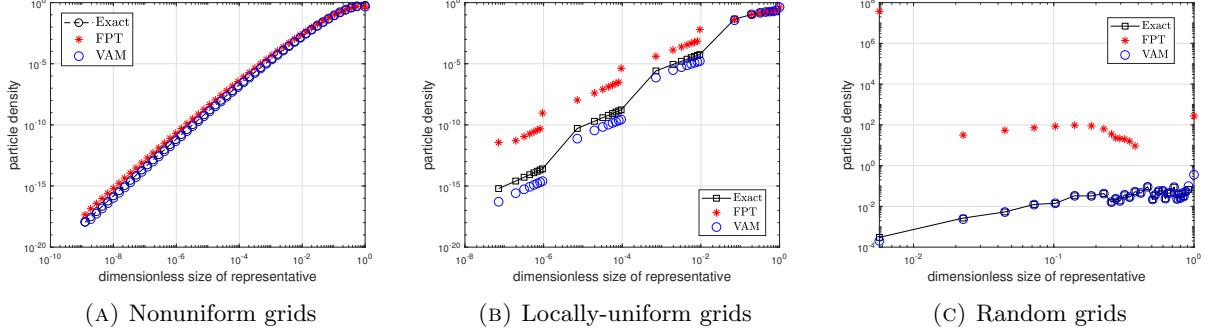(A) Nonuniform grids   (B) Locally-uniform grids   (C) Random grids

FIGURE 10. Comparison of number density for different grid types at $t = 1$ for test case 5.2.

The first two moments are predicted with high accuracy by both the methods (refer to Figure 11a and Table 2) for nonuniform grids. For second order moment VAM generates less error and gives better prediction as compared to FPT. A similar observation can be made from the Table 2.
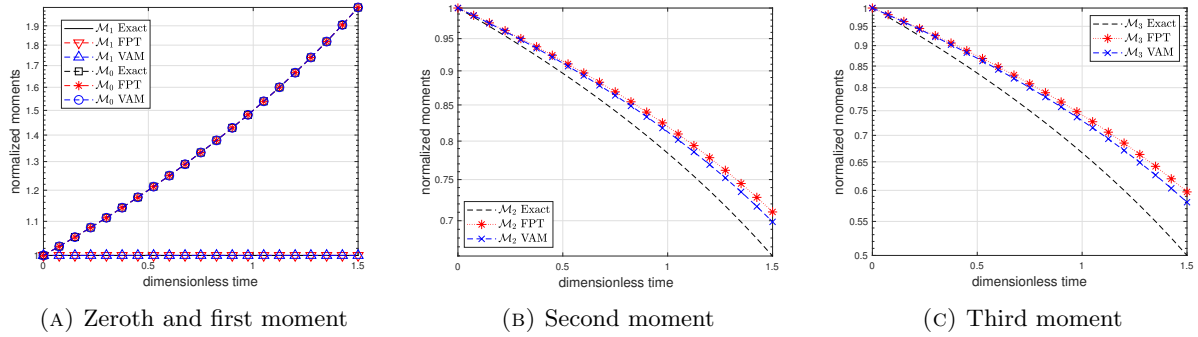

(A) Zeroth and first moment   (B) Second moment   (C) Third moment

FIGURE 11. Different order moments for test case 5.2.

Method	VAM			FPT		
Time	$E_{\mathcal{M}_0}$	$E_{\mathcal{M}_1}$	$E_{\mathcal{M}_2}$	$E_{\mathcal{M}_0}$	$E_{\mathcal{M}_1}$	$E_{\mathcal{M}_2}$
0.3	$2.57{\times}10^{-11}$	$1.45{\times}10^{-11}$	$1.21{\times}10^{-2}$	$2.57{\times}10^{-11}$	$1.45{\times}10^{-11}$	$1.01{\times}10^{-2}$
0.6	$4.94{\times}10^{-11}$	$1.42{\times}10^{-11}$	$2.07{\times}10^{-2}$	$4.94{\times}10^{-11}$	$1.42{\times}10^{-11}$	$2.53{\times}10^{-2}$
0.9	$4.63{\times}10^{-11}$	$6.63{\times}10^{-11}$	$3.22{\times}10^{-2}$	$4.63{\times}10^{-11}$	$6.63{\times}10^{-11}$	$4.02{\times}10^{-2}$
1.2	$3.47{\times}10^{-10}$	$2.26{\times}10^{-10}$	$4.48{\times}10^{-2}$	$3.47{\times}10^{-10}$	$2.26{\times}10^{-10}$	$5.71{\times}10^{-2}$
1.5	$7.72{\times}10^{-10}$	$3.19{\times}10^{-10}$	$5.90{\times}10^{-2}$	$7.72{\times}10^{-10}$	$3.19{\times}10^{-10}$	$7.67{\times}10^{-2}$

TABLE 2. Error analysis of different order moments for test case 5.2.

5.2. **Experimental order of convergence.** The theoretical results demonstrating the order of convergence of the new scheme VAM are examined against the numerical estimated order of convergence (EOC) for analytically tractable kernels [11] using the following formula:

$$(5.2) \qquad \text{EOC} = \frac{\ln\left(\dfrac{E_I}{E_{2I}}\right)}{\ln(2)},$$

where E_I is the L^1 error norm calculated by

$$(5.3) \qquad E_I := \sum_{j=1}^{I} |N_j - \hat{N}_j| = ||N - \hat{N}|| \quad \text{and} \quad L^1_{\text{error}} := \frac{||N - \hat{N}||}{||N||} = \frac{E_I}{||N||}.$$

Here, the subscript I corresponds to the degrees of freedom. The EOC is calculated for all the test cases considered for uniform, nonuniform, locally-uniform and random grids (see Table 3 and 4). For calculating the EOC, computation size domain $[10^{-9}, 1]$ is considered, which is discretized into 30 grids initially. These grids are doubled in each iteration and five iterations are performed. EOC is calculated over four different grid types, namely uniform, nonuniform, locally-uniform and random. For all simulations end time considered as $t = 1$.

TABLE 3. L^1 error and EOC for test case 5.1 for VAM.

	Nonuniform grids		Uniform grids		Locally-uniform grids		Random grids	
Grids	L^1 error	EOC	L^1 error	EOC	L^1 error	EOC	L^1 error	EOC
30	0.97×10^{-1}	0	3.56×10^{-2}	0	8.25×10^{-1}	0	3.59×10^{-1}	0
60	4.55×10^{-1}	1.16	1.71×10^{-2}	1.05	2.31×10^{-1}	1.18	2.28×10^{-1}	0.57
120	2.03×10^{-1}	1.11	8.36×10^{-3}	1.03	1.07×10^{-1}	1.10	1.53×10^{-1}	0.65
240	9.34×10^{-2}	1.09	4.13×10^{-3}	1.01	4.91×10^{-2}	1.11	9.35×10^{-2}	0.72
480	4.45×10^{-2}	1.06	2.05×10^{-3}	1.01	2.31×10^{-2}	1.08	5.81×10^{-2}	0.87

TABLE 4. L^1 error and EOC for test case 5.2 for VAM.

	Nonuniform grids		Uniform grids		Locally-uniform grids		Random grids	
Grids	L^1 error	EOC	L^1 error	EOC	L^1 error	EOC	L^1 error	EOC
30	6.21×10^{-1}	0	6.32×10^{-2}	0	6.66×10^{-1}	0	6.32×10^{-2}	0
60	3.97×10^{-1}	0.65	3.19×10^{-2}	1.00	2.42×10^{-1}	0.76	5.34×10^{-2}	0.67
120	2.24×10^{-1}	0.82	1.59×10^{-2}	1.00	1.42×10^{-1}	0.84	2.64×10^{-2}	0.76
240	1.25×10^{-1}	0.84	8.07×10^{-3}	0.99	7.91×10^{-2}	0.94	1.41×10^{-2}	0.85
480	6.74×10^{-2}	0.89	4.03×10^{-3}	0.99	4.12×10^{-2}	0.97	1.02×10^{-2}	0.89

Table 3 presents the L^1 error and EOC data for different grid types for Example 5.1. It can be observed from the data that VAM is first order accurate irrespective of grid choice. For the first three type of grids, the convergence order is achieved rapidly, however for random grids, it is convergence is comparatively slow to other grids. It is interesting to note that for all the grids, L^1 error is decreasing by half when the number of grids are doubled. For Example 5.2, Table 4 contains the data for L^1 error and EOC. Similar to previous case, first order of convergence is noticed for all four grid types.

Therefore, by numerical experiments we can say that the VAM performs accurately and predict the convergence results with better accuracy in comparison with existing FPT [11].

Remark 5.1. Here, we verify the claim made in Remark 3.4. Consider $\beta(x|y; z) = \dfrac{12x}{y^2}\left(1 - \dfrac{x}{y}\right)$ and calculate the EOC for VAM over uniform, nonuniform, locally-uniform and random grids. Table 5 supports the claim.

TABLE 5. L^1 error and EOC for VAM with $\beta(x|y; z) = \dfrac{12x}{y^2}\left(1 - \dfrac{x}{y}\right)$.

	Nonuniform grids		Uniform grids		Locally-uniform grids		Random grids	
Grids	L^1 error	EOC	L^1 error	EOC	L^1 error	EOC	L^1 error	EOC
30	2.45×10^{-2}	0	1.06×10^{-0}	0	9.92×10^{-1}	0	2.41×10^{-2}	0
60	7.24×10^{-3}	1.77	4.14×10^{-1}	1.35	2.11×10^{-1}	2.23	1.89×10^{-2}	0.85
120	2.06×10^{-3}	1.85	1.33×10^{-1}	1.63	6.57×10^{-2}	1.68	8.39×10^{-3}	1.18
240	5.76×10^{-4}	1.91	3.79×10^{-2}	1.81	1.65×10^{-2}	1.99	4.25×10^{-3}	0.98
480	1.75×10^{-4}	1.94	1.01×10^{-2}	1.91	4.21×10^{-3}	1.98	2.87×10^{-3}	1.08

5.3. Two-dimensional case.

Test case 5.3. *Consider multi-dimensional collisional nonlinear breakage equation with monodispresed initial condition with collisional kernel* $\mathcal{K}(x_1, x_2, y_1, y_2) = x_1 x_2 y_1 y_2$ *and breakage function as* (i) $\beta(x_1, x_2|y_1, y_2; z_1, z_2) = \dfrac{4}{y_1 y_2}$ *and* (ii) $\beta(x_1, x_2|y_1, y_2; z_1, z_2) = \dfrac{2}{y_1 y_2}$.

Case (i): For this case, exact zeroth $\mathcal{M}_{0,0}(t)$ and first moment $\mathcal{M}_{1,1}(t)$ can be calculated. However, the total amount of property with respect to x_1 and x_2 or first cross moments $\mathcal{M}_{0,1}(t)$ and $\mathcal{M}_{1,0}(t)$ are unavailable. In Figure 12a zeroth moment and hypervolume are plotted and compared against the exact values. An excellent prediction of both the integral properties can be noticed. The total of first order mixed moments is showcased in Figure 12b. The prediction of average hypervolume depends on the zeroth and hypervolume as it is defined as their ratio. A high accurate approximation of averaged value is anticipated and shown in Figure 12c.

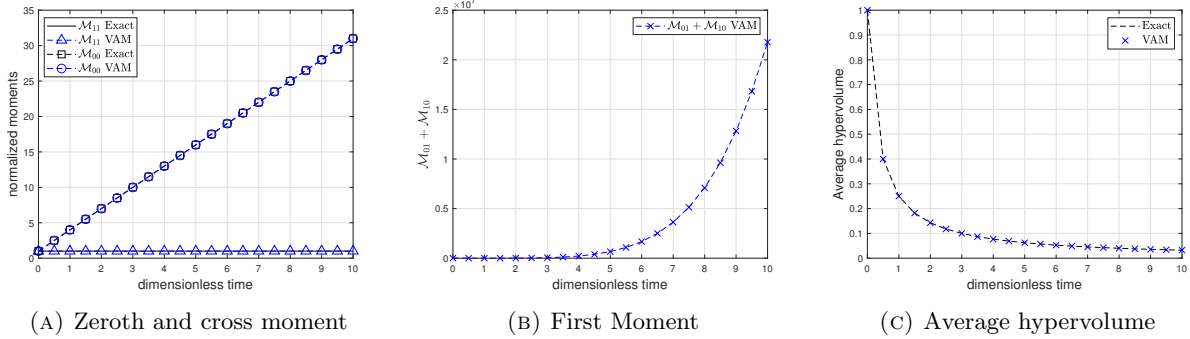(A) Zeroth and cross moment   (B) First Moment   (C) Average hypervolume

FIGURE 12. Comparison of different order moments for multi-dimensional model.

Case (ii): On contrast to previous case, in this case first order mixed moments are conserved and zeroth and cross moments are calculated exactly. Figure 13a presents the zeroth and first cross moment. The mixed moments are conserved, when VAM is used as depicted in Figure 13b. Finally, average hypervolume is plotted in Figure 13c.

(A) Zeroth and cross moemnt   (B) First Moment   (C) Average hypervolume
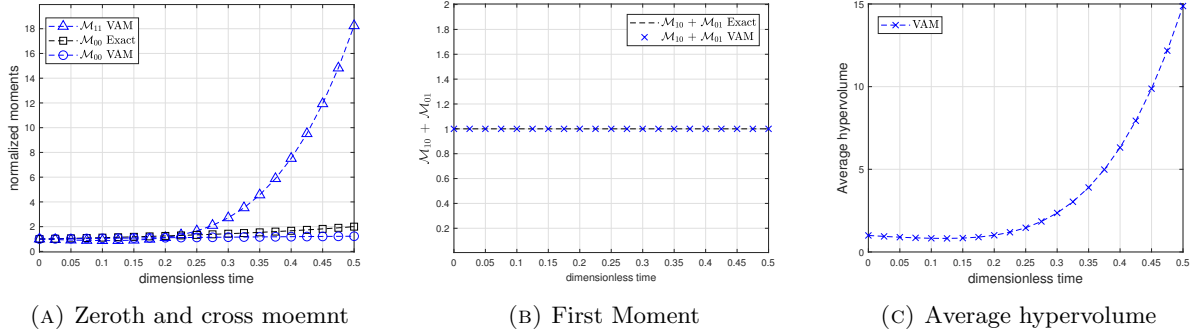
FIGURE 13. Comparison of different order moments for multi-dimensional model.

6. CONCLUSION

This study provided a comprehensive stability and consistency analysis of the new scheme volume average method for the collisional nonlinear breakage equation. It documented the mathematical and numerical results in comparison with the existing scheme fixed pivot techniques. It is noteworthy that the new scheme achieves first order convergence rate over random grids, whereas the existing scheme fixed pivot techniques are inconsistent over random grids. Moreover, it is shown that the new scheme is first order convergence rate over oscillatory grids. Furthermore, our considered equation is extended for two-dimensional case over rectangular grids. Most importantly, numerical experiments have been performed successfully for one and two-dimensional collisional nonlinear breakage equation with two test examples for each case. Additionally, we explored a detailed error estimation for the new scheme.

7. ACKNOWLEDGEMENT

8. CONFLICT OF INTEREST STATEMENT

All the authors certify that they do not have any conflict of interest.

9. DATA AVAILABILITY STATEMENT

The data that support the findings of this study is available from the corresponding author upon reasonable request.

REFERENCES

1. Z Cheng and S Redner, *Scaling theory of fragmentation*, Physical Review Letters **60** (1988), no. 24, 2450.
2. _____, *Kinetics of fragmentation*, Journal of Physics A: Mathematical and General **23** (1990), no. 7, 1233.
3. Arijit Das, Prakrati Kushwah, Jitraj Saha, and Mehakpreet Singh, *Improved higher-order finite volume scheme and its convergence analysis for collisional breakage equation*, Applied Numerical Mathematics **196** (2024), 118–132. MR 4666144
4. Arijit Das and Jitraj Saha, *Approximate solutions to the nonlinear hyperbolic population balance equation: convergence, error estimate and numerical simulations*, Zeitschrift Für Angewandte Mathematik und Physik **75** (2024), no. 4, 125.
5. Ashok Das, Jitendra Kumar, Maksym Dosta, and Stefan Heinrich, *On the approximate solution and modeling of the kernel of nonlinear breakage population balance equation*, SIAM Journal on Scientific Computing **42** (2020), no. 6, B1570–B1598.
6. Ankik Kumar Giri, Ram Gopal Jaiswal, and Philippe Laurençot, *The continuous collision-induced nonlinear fragmentation equation with non-integrable fragment daughter distributions*, Journal of Differential Equations **403** (2024), 235–271.
7. Ankik Kumar Giri and Philippe Laurençot, *Weak solutions to the collision-induced breakage equation with dominating coagulation*, Journal of Differential Equations **280** (2021), 690–729.
8. Jitendra Kumar, Jitraj Saha, and Evangelos Tsotsas, *Development and convergence analysis of a finite volume scheme for solving breakage equation*, SIAM Journal on Numerical Analysis **53** (2015), no. 4, 1672–1689.
9. Jitendra Kumar and Gerald Warnecke, *Convergence analysis of sectional methods for solving breakage population balance equations-I: The fixed pivot technique*, Numerische Mathematik **111** (2008), 81–108.

10. _____, *Convergence analysis of sectional methods for solving breakage population balance equations-II: The cell average technique*, Numerische Mathematik **110** (2008), 539–559.

11. Prakrati Kushwah, Arijit Das, Jitraj Saha, and Andreas Bück, *Population balance equation for collisional breakage: a new numerical solution scheme and its convergence*, Communications in Nonlinear Science and Numerical Simulation **121** (2023), Paper No. 107244, 20. MR 4566091

12. Prakrati Kushwah and Jitraj Saha, *Performance analysis and accuracy of numerical methods for solving simultaneous nonlinear particulate processes with multi-dimensional extension*, Proceedings A, vol. 480, The Royal Society, 2024, p. 20240293.

13. O₋ Levenspiel, D Kunii, and T Fitzgerald, *The processing of solids of changing size in bubbling fluidized beds*, Powder Technology **2** (1968), no. 2, 87–96.

14. SI Piotrowski, *The collisions of asteroids*, Acta Astronomica **6** (1953), 115–138.

15. Olivier P Prat, Ana P Barros, and Firat Y Testik, *On the influence of raindrop collision outcomes on equilibrium drop size distributions*, Journal of the Atmospheric Sciences **69** (2012), no. 5, 1534–1546.

16. Jitraj Saha and Mehakpreet Singh, *Rate of convergence and stability analysis of a modified fixed pivot technique for a fragmentation equation*, Numerische Mathematik **153** (2023), no. 2, 531–555.

17. Mehakpreet Singh, Saeed Shirazian, Vivek Ranade, Gavin M Walker, and Ashish Kumar, *Challenges and opportunities in modelling wet granulation in pharmaceutical industry–a critical review*, Powder Technology **403** (2022), 117380.

18. R Dennis Vigil, Isaac Vermeersch, and Rodney O Fox, *Destructive aggregation: Aggregation with collision-induced breakage*, Journal of Colloid and Interface Science **302** (2006), no. 1, 149–158.

19. Nisha Yadav, Ashok Das, Mehakpreet Singh, Sukhjit Singh, and Jitendra Kumar, *Homotopy perturbation method and its convergence analysis for nonlinear collisional fragmentation equations*, Proceedings of the Royal Society A **479** (2023), no. 2279, 20230567.

A. Derivation of equation (2.21) in Proposition 2.1:

We have to prove the expression

$$\sum_{i=1}^{I} x_i \hat{B}_{i-1} \lambda_i^-(\bar{v}_{i-1}) H(\bar{v}_{i-1} - x_{i-1}) + \sum_{i=1}^{I} x_i \hat{B}_i \lambda_i^-(\bar{v}_i) H(x_i - \bar{v}_i) + \sum_{i=1}^{I} x_i \hat{B}_i \lambda_i^+(\bar{v}_i) H(\bar{v}_i - x_i)$$

$$\text{(A.1)} \qquad + \sum_{i=1}^{I} x_i \hat{B}_{i+1} \lambda_i^+(\bar{v}_{i+1}) H(x_{i+1} - \bar{v}_{i+1}) = \sum_{i=1}^{I} \bar{v}_i \hat{B}_i$$

Proof.

$$\frac{\mathrm{d}}{\mathrm{d}t} \sum_{i=1}^{I} x_i \hat{N}_i(t) = \sum_{i=1}^{I} x_i \hat{B}_{i-1} \lambda_i^-(\bar{v}_{i-1}) H(\bar{v}_{i-1} - x_{i-1}) + \sum_{i=1}^{I} x_i \hat{B}_i \lambda_i^-(\bar{v}_i) H(x_i - \bar{v}_i)$$

$$+ \sum_{i=1}^{I} x_i \hat{B}_i \lambda_i^+(\bar{v}_i) H(\bar{v}_i - x_i) + \sum_{i=1}^{I} x_i \hat{B}_{i+1} \lambda_i^+(\bar{v}_{i+1}) H(x_{i+1} - \bar{v}_{i+1})$$

$$\text{(A.2)} \qquad - \sum_{i=1}^{I} \sum_{j=1}^{I} x_i \mathcal{K}(x_i, x_j) \hat{N}_i(t) \hat{N}_j(t).$$

If $v_i > x_i$, then the above equation is written as

$$\frac{\mathrm{d}}{\mathrm{d}t} \sum_{i=1}^{I} x_i \hat{N}_i(t) = \sum_{i=1}^{I} x_i \hat{B}_{i-1} \lambda_i^-(\bar{v}_{i-1}) + \sum_{i=1}^{I} x_i \hat{B}_i \lambda_i^+(\bar{v}_i) - \sum_{i=1}^{I} \sum_{j=1}^{I} x_i \mathcal{K}(x_i, x_j) \hat{N}_i(t) \hat{N}_j(t)$$

$$= \sum_{i=1}^{I} x_{i+1} \hat{B}_i \lambda_{i+1}^-(\bar{v}_i) + \sum_{i=1}^{I} x_i \hat{B}_i \lambda_i^+(\bar{v}_i) - \sum_{i=1}^{I} \sum_{j=1}^{I} x_i \mathcal{K}(x_i, x_j) \hat{N}_i(t) \hat{N}_j(t)$$

$$= \sum_{i=1}^{I} \left(x_{i+1} \lambda_i^-(\bar{v}_i) + x_i \lambda_i^+(\bar{v}_i) \right) \hat{B}_i - \sum_{i=1}^{I} \sum_{j=1}^{I} x_i \mathcal{K}(x_i, x_j) \hat{N}_i(t) \hat{N}_j(t)$$

$$= \sum_{i=1}^{I} \left(x_{i+1} \frac{\bar{v}_i - x_i}{x_{i+1} - x_i} + x_i \frac{\bar{v}_i - x_{i+1}}{x_i - x_{i+1}} \right) \hat{B}_i - \sum_{i=1}^{I} \sum_{j=1}^{I} x_i \mathcal{K}(x_i, x_j) \hat{N}_i(t) \hat{N}_j(t)$$

$$\text{(A.3)} \qquad = \sum_{i=1}^{I} \bar{v}_i \hat{B}_i - \sum_{i=1}^{I} \sum_{j=1}^{I} x_i \mathcal{K}(x_i, x_j) \hat{N}_i(t) \hat{N}_j(t).$$

By similar argument for $v_i < x_i$, we have

$$(A.4) \qquad \frac{\mathrm{d}}{\mathrm{d}t} \sum_{i=1}^{I} x_i \hat{N}_i(t) = \sum_{i=1}^{I} \bar{v}_i \hat{B}_i - \sum_{i=1}^{I} \sum_{j=1}^{I} x_i \mathcal{K}(x_i, x_j) \hat{N}_i(t) \hat{N}_j(t).$$

$\square$

Department of Mathematics, National Institute of Technology Tiruchirappalli, Tamil Nadu - 620 015, India.
Email address: kprakrati1256@gmail.com

Department of Mathematics, National Institute of Technology Tiruchirappalli, Tamil Nadu - 620 015, India.
Email address: anupamaghorai@gmail.com

Department of Mathematics, National Institute of Technology Tiruchirappalli, Tamil Nadu - 620 015, India.
Email address: jitraj@nitt.edu (Corresponding author)